THERMODYNAMIC ANALYSIS OF THE ABSORPTION ENHANCED STEAM REFORMING OF BIOFUEL MODEL COMPOUNDS

Miguel A. Escobedo Bretado[1], Manuel D. Delgado Vigil[2], Jesús Salinas Gutiérrez[2], Miguel Meléndez Zaragoza[2], Virginia Collins-Martínez[2] and Alejandro López Ortiz[2]

[1] Facultad de Ciencias Químicas, Universidad Juárez del Estado de Durango, Ave. Veterinaria s/n, Circuito Universitario, Durango 34120, México
[2] Departamento de Materiales Nanoestructurados, Centro de Investigación en Materiales Avanzados, S.C. Miguel de Cervantes 120, Chihuahua, Chih. 31109, México,
[*] contact email: alejandro.lopez@cimav.edu.mx

ABSTRACT

Thermodynamic analysis of the steam reforming of biofuel model compounds using CaO, CaO*MgO, Na_2ZrO_3, Li_2ZrO_3 and Li_4SiO_4 as CO_2 absorbents was performed to determine favorable operating conditions to produce a high hydrogen ratio (HR) and concentration (% H_2) gas product. Biofuel compounds (HC's) used were: 2,4-dimethylphenol (DMP), furfural (FUR) and vanillin (VAI). Equilibrium product compositions were studied at temperature (300-850°C), steam to hydrocarbon molar feed ratio (S/HC) and type of CO_2 absorbent at 1 atm. S/HC varied from stoichiometric; 15:1 for DMP, 13:1 for VAI and 8:1 for FUR to twice and trice their stoichiometric values, respectively. At stoichiometric S/HC ratios results indicate significant carbon formation with conventional reforming at T < 600°C. However, no carbon formation was found using absorbents with any of the HC's. The use of a CO_2 absorbent resulted in an increase in HR (molsH_2/molHC fed) and H_2 purity of about 3 and 30% higher, respectively. For most of HC's CaO and CaO*MgO showed similar results with an HR of 7 and 90% H_2, Na_2ZrO_3 and Li_2ZrO_3 resulted only in slightly lower values than CaO, while Li_4SiO_4 showed significantly lower values than CaO. The order from higher to lower HR based on model molecule was: VA>DMP>FUR. Na_2ZrO_3 should be considered as high potential absorbent in the system due to its superior thermal stability and kinetics.

Keywords: Absorption-Enhanced-Reforming, Biofuel, CO_2-absorbent, thermodynamic analysis

1. INTRODUCTION

Considering the fact that energy consumption is increasing and limited fossil fuels are nearly exhausted, with increasing population and economic development, renewable energy must be widely explored in order to renew energy sources and keep sustainable development safe [1].

Biomass-based feedstocks have recently gained significant interest. For example, the use of biomass resources such as agricultural wastes and fast growing lignocellulosic raw materials are currently being recognized as attractive options due to their renewable, reliable and CO_2-neutral features [2].

For many years, fossil fuels have played an important role in the traditional hydrogen production process. But the depletion of natural fossil fuel reserves, constant price rising and serious environmental problems drive researchers to focus more on hydrogen production from renewable energy sources. Renewable energy sources should be clean and not expected to run out by reasonable utilization. Because of their consistent long-term availability, renewable energy resources are also inherently more stable in price than fossil fuels [3].

Hydrogen and electricity can be one of the key solutions for the 21st century, enabling clean efficient production of power and heat from a wide range of primary energy sources. Today, hydrogen is mainly produced from natural gas via steam methane reforming, a process suffering from several problems like thermodynamic equilibrium limitations, high energy demand, catalyst deactivation due to carbon deposition and increased CO_2 emissions. Considerable research efforts have been also directed to the production of hydrogen via partial oxidation and CO_2 reforming. Since the above mentioned processes rely on a non-renewable fossil fuel, they are not a viable long-term source of hydrogen [4].

Moreover, hydrogen as a clean fuel has attracted great attention worldwide in recent years. Its production from renewable energy sources such as biomass can reduce emissions of SO_2 and

NOx's remarkably, and in addition, a CO_2 neutral energy supply can be achieved [5]. A zero net emission of CO_2 can be achieved because it's released from biomass will be recycled into the plants by photosynthesis. The energy crisis and fuel demand made biomass and fast pyrolysis liquefaction a very important area of research and development. Hydrogen can be produced by combining the steam reforming of biomass and the water-gas shift reaction. However, with regard to biomass itself, its low energy density always leads to high transportation costs, and therefore, hydrogen production from biomass on a large scale will be economically limited.

Conversely, Bio-oil produced from fast pyrolysis of biomass represents a type of high-energy density chemical and a uniform feedstock that has much higher energy density than that of biomass, which could be transported easily from scattered collection stations to a large scale processing plant [4, 5]. Therefore catalytic steam reforming of bio-oil will be one of the most promising and economically viable methods for hydrogen production

Generally speaking, the liquid product from biomass pyrolysis is known as biomass pyrolysis oil, bio-oil, pyrolysis oil, or bio-crude. Bio-oils are derived from depolymerization and fragmentation of cellulose, hemicellulose and lignin. They are a complex mixture, highly oxygenated with a great amount of large size molecules, which nearly involve all species of oxygenated organics, such as esters, ethers, aldehydes, ketones, phenols, carboxylic acids and alcohols. Bio-oil can be divided in two fractions: a carbohydrate fraction (water soluble) and a lignin-derived fraction (water insoluble). The remaining water-rich carbohydrate fraction can be steam reformed over a catalyst to generate hydrogen or be used as a fuel in heat and power generation. Furthermore, its conversion to syngas by mechanisms such as steam reforming and partial oxidation offers a sustainable way of synthesizing value added chemicals [2]. Also, it can be considered that 99.7% of bio-oil is formed by a complex mixture of carbon, hydrogen and oxygen. For example the bio-oil from *P. indicus* (wood source) is mainly comprised of levoglucosan, furfural, phenols, aldehydes and vanillin [1].

On the other hand, a new concept involving simultaneous hydrogen production and carbon dioxide removal has been proposed and developed [6-9]. The utilization of a CO_2 absorbent in the reforming reactor sharply decreases the CO_2 level in the reacting gas and shifts the equilibrium towards hydrogen production. This makes possible high fuel conversion at relatively low temperatures and production of high-quality hydrogen *(~ 95%)* with only traces of carbon oxides (in the order of 1 vol%). This concept has been called absorption enhanced steam reforming (AESR). This AESR process provides an alternative for a single step high purity hydrogen production [10]. The fundamental concept of this process is based in the Le Chatellier's principle in which the reaction equilibrium can be shifted towards the production of hydrogen when CO_2 is removed *in situ* within the reforming reactor. Thus, if the carbon dioxide generated during the steam reforming step is removed from the gas phase using a solid CO_2 absorbent such as CaO the hydrogen production will be enhanced. Recent experiments by Yi and Harrison [11] demonstrated that in the presence of an absorbent fairly good conversion and very low concentrations of CO can be achieved even at very low pressures (1 bar) and low temperatures (460°C). A potential absorbent material should have good absorption capacity at high temperatures, should be easily regenerable and thermally stable to allow a cyclic absorption–desorption process. Experimental studies have demonstrated that CaO is able to generate high H_2 concentrations by steam reforming of methane under absorption-enhanced steam reforming (AESR) process concept [7, 8].

In the AESR reactor a mixture of a CO_2 absorbent (for example CaO) and a reforming catalyst will theoretically produce a high purity hydrogen stream in one single step. CO_2 absorption by CaO can be achieved through the reaction:

$$CaO + CO_2(g) = CaCO_3 \qquad \Delta H°_{298} = -178.3 \text{ kJ/mol} \qquad (1)$$

However, this absorbent must be regenerated if a continuous process is desired and then the high endothermic reverse reaction (1) will eventually be required to be performed. Recent studies have

developed synthetic CO_2 absorbents. Compounds such as: lithium orthosilicate (Li_4SiO_4), lithium zirconate (Li_2ZrO_3) [12] and sodium zirconate (Na_2ZrO_3) [13], which are able to withstand many carbonation/regeneration cycles without important loss of capacity and activity at high temperatures. Therefore, these synthetic absorbents have become highly attractive to be used under the proposed AESR process.

Moreover, Kinoshita and Turn [14] investigated the thermodynamics of the sorption enhanced reforming of bio-oil and evaluated an overall process for production of high-purity hydrogen using the ASPEN PLUS process simulator. They modeled the bio oil AERS using CaO as CO_2 absorbent and dextrose ($C_6H_{12}O_6$) as a model molecule and found that by operating the reformer in a temperature range of 600–750◦C and the desorbing (regeneration) reactor at ∼ 800◦C at atmospheric pressure a gas product containing > 95% H_2 can be produced. Also, Iordanidisa et al. [15] investigated the thermodynamic modeling of the sorption-enhanced steam reforming of bio-oil/biogas for electricity and heat generation by phosphoric acid fuel cells, using the SIMSCI Pro II process simulator. They also used CaO as a CO_2 absorbent, with a mixture of typical bio oil compounds; acetic acid ($C_2H_4O_2$), acetone (C_3H_6O), acetaldehyde (C_2H_4O), ethylene glycol ($C_2H_6O_2$), formic acid (CH_2O_2), methanol (CH_4O), formaldehyde (CH_2O) and ethanol (C_2H_6O).

For simulation purposes, it is a difficult matter to choose a model molecule to study the steam reforming thermodynamics of bio oil. Due to the complex nature of this, its behavior in conversion to syngas has been represented by the conversion of appropriate model compounds such as acetic acid [16–21], acetone [16,4, 22, 23], dibenzyl ether [19], ethyl lactate [23], ethyl propionate [24], ethylene glycol [4,23,24], hydroxyacetaldehyde [20], glycerol [23,25], glucose [18,19], lactic acid [19], m-cresol [18,26], phenol [16], propioanic acid [19], sorbitol [23], sucrose [18], xylose [18] and ethanol [27]. However the present study makes use of main compounds in organic composition of bio-oil produced from *Penaeus. Indicus* (indian prawn wood), which is one of the major commercial prawn species of the world. Mayor components in

the bio oil produced from this wood are: furfural (FUR), 2,4-dimethyl phenol (DMP) and vanillin (VAI) [1].

In the present study, a thermodynamic analysis of steam reforming of FUR, DMP and VAI, with and without the use of a CO_2 absorbent was carried out to determine favorable operating conditions to produce a high purity hydrogen gas product. The CO_2 absorbents studied were; CaO, CaO*MgO, Na_2ZrO_3, Li_2ZrO_3 and Li_4SiO_4. The influence of steam-to-fuel feed molar ratio and temperature on the product gas concentration was investigated for all cases. Also, in the AESR reaction system, pressure was kept at atmospheric conditions. Furthermore, it is expected that during the steam reforming of the model molecules, carbon deposition over catalysts may be the main cause for deactivation, resulting in low durability and activity loss. Therefore, additionally a study of conditions where this carbon deposition is expected with and without the use of a CO_2 absorbent is presented.

2. SIMULATION CALCULATIONS

2.1 Gibbs Free Energy Minimization Technique

In a reaction system where many simultaneous reactions take place, equilibrium calculations can be performed through the Gibbs energy minimization approach (also called the non-stoichiometric method). In this technique the total free energy of the system consisting of an ideal gas phase and pure condensed phases, can be expressed as:

$$\frac{G}{RT} = \left\{ \sum_{i=1}^{N} n_i \frac{G_i^{\circ}}{RT} + \ln\left(y_i P\right) \right\}_{gas} + \frac{1}{RT} \left\{ \sum_{i=1}^{N} n_i \, G_i^{\circ} \right\}_{condensed} \quad (2)$$

The technique is based in finding different values of n_i which minimizes the objective function (2) and subjected to the constraints of the elemental mass balance:

$$\sum_{i=1}^{N} a_{ij}\, n_i = A_j, \quad j = 1, 2, 3 \ldots, k \qquad (3)$$

where a_{ij} is the number of atoms of the j^{th} element in a mole of the i^{th} species. A_j is defined as the total number of atoms of the j^{th} element in the reaction mixture [28]. All calculations were performed through the use of the equilibrium module of the HSC chemistry software [29]. HSC calculates the equilibrium composition of all possible combination of reactions that are able to take place within the thermodynamic system. These equilibrium calculations make use of the equilibrium composition module of the HSC program that is based on the Gibbs free energy minimization technique. The GIBBS program of this module finds the most stable phase combination and seeks the phase compositions where the Gibbs free energy of the system reaches its minimum (equation 2) at a fixed mass balance (a constraint minimization problem, equation 3), constant pressure and temperature.

In this non-stoichiometric approach every species in the system must be defined. The selection of feasible products should be based on previous experimental results found in the literature. For each system the possible species are specified based on reported experimental and thermodynamic analysis studies. In the steam reforming of bio oil system the included species were: acetic acid, acetone, dibenzyl ether, ethyl lactate, ethyl propionate, ethylene glycol, hydroxyl acetaldehyde, glycerol, glucose, lactic acid, m-cresol, phenol, propionic acid, sorbitol, sucrose, xylose, C, CO, CH_4, CO_2, H_2, and H_2O. All these compounds were based on reported experimental species found in the literature [16-27]. Identical conditions were used for the cases where a CO_2 absorbent was included, with the exception that two solid phases were added; solid absorbents and elemental carbon. In the case of CO_2 absorbent CaO, the species $Ca(OH)_2$ and $CaCO_3$ were added. For dolomite were: CaO*MgO, CaO, $CaCO_3$, $MgCO_3$ and MgO. For sodium zirconate were: Na_2ZrO_3, Na_2CO_3 and ZrO_2. For lithium zirconate were: Li_2ZrO_3, Li_2CO_3 and ZrO_2 and finally for lithium orthosilicate were: Li_4SiO_4, Li_2CO_3 and Li_2SiO_3. All of these correspond to the following carbonation reactions:

$CaO*MgO + CO_2(g) = CaCO_3 + MgO$ $\Delta H°_{298} = -170.9$ kJ/mol (4)

$Na_2ZrO_3 + CO_2(g) = Na_2CO_3 + ZrO_2$ $\Delta H°_{298} = -151.5$ kJ/mol (5)

$Li_2ZrO_3 + CO_2(g) = Li_2CO_3 + ZrO_2$ $\Delta H°_{298} = -162.5$ kJ/mol (6)

$Li_4SiO_4 + CO_2(g) = Li_2CO_3 + Li_2SiO_3$ $\Delta H°_{298} = -142.2$ kJ/mol (7)

During the simulation work the reaction temperature was varied in the range of 300-850°C at 1 atm. The steam reforming for FUR, DMP and VAI are represented by the following reactions:

$C_5H_4O_2$ (FUR) $+ 8H_2O(g) = 5CO_2(g) + 10H_2(g)$ $\Delta H°_{298} = 115.5$ kJ/mol (9)

$C_8H_{10}O$ (DMP) $+ 15H_2O(g) = 8CO_2(g) + 20H_2(g)$ $\Delta H°_{298} = 703.0$ kJ/mol (10)

$C_8H_8O_3$ (VAI) $+ 13H_2O(g) = 8CO_2(g) + 17H_2(g)$ $\Delta H°_{298} = 359.9$ kJ/mol (11)

The stoichiometric steam needed for each reaction was settled based upon reactions (9) to (11). Steam to hydrocarbon molar feed ratio (S/HC) was then varied from stoichiometric; 8:1 for FUR, 15:1 for DMP and 13:1 for VAI to twice and trice their stoichiometric values, respectively.

All the previous description of the simulation calculations is based on theoretical thermodynamic considerations and these are to be taken as a guide to further experimental evaluation of the reaction systems, since no heat and mass diffusional limitations as well as kinetics effects were taken into account for the conformation of the present thermodynamic analysis.

2. RESULTS AND DISCUSSION

2.1 Thermodynamically Possible Products

According to recent results from bio-oil steam reforming combined with CO_2 absorbents [30-32] main gaseous species present in the effluent of the reactor were CO, CO_2, CH_4 and H_2, with only traces of other organic compounds already described in section 1. Therefore for the present thermodynamic analysis only the main gaseous species were considered, since after calculations

of steam reforming for FUR, DMP and VAI other byproduct species presented negligible concentrations at equilibrium. In practice steam reforming reactions of the above referenced studies are under kinetic control, where suitable catalysts and supports are able to completely convert all the bio oils to avoid intermediate products. All this agrees well with the fact that only trace amounts (less than 1ppm) of these oxygenated intermediates were found in all the thermodynamic calculations performed and therefore these were not reported in the present study.

2.2 Furfural Steam Reforming System

Figure 1 presents the effects of temperature, steam to furfural molar feed ratio (S/FUR) on the hydrogen production rate (HY, defined as mols of H_2 produced per mol of furfural fed to the system) and H_2 dry basis gas concentration (% H_2) in the product. This HR is a criterion to quantitatively compare different reactions systems (with and without a CO_2 absorbent) for the hydrogen production at equilibrium.

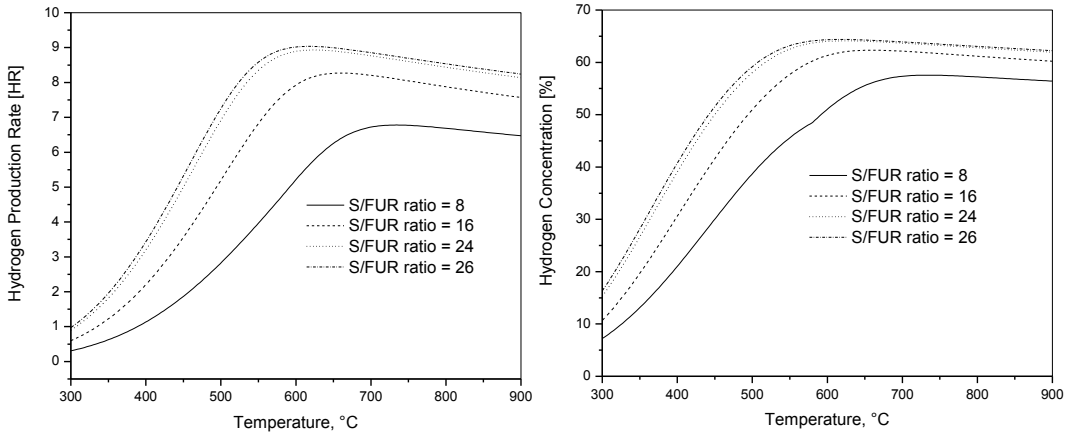

Figure 1. Equilibrium HR and H_2 for Furfural Steam Reforming.

The S/FUR was varied from 8:1 (stoichiometric) to 26:1 in a temperature range of 300-900°C. In this conventional system the production of CO and H_2 are higher as temperature increases, since low temperatures generate low CO and H_2 (as low as 7.2% H_2 at 300°C). At these (T = 300°C) same conditions CO_2 (48%) and CH_4 (44%) are the predominant gaseous species.

These results can be explained by the following methanation reactions:

$2CO(g) + 2H_2(g) = CH_4(g) + CO_2(g)$ $\Delta H°_{298} = -247.4$ kJ/mol (12)

$CO_2(g) + 4H_2(g) = CH_4(g) + 2H_2O(g)$ $\Delta H°_{298} = -169.9$ kJ/mol (13)

$CO(g) + 3H_2(g) = CH_4(g) + H_2O(g)$ $\Delta H°_{298} = -206.2$ kJ/mol (14)

$C(s) + 2H_2(g) = CH_4(g)$ $\Delta H°_{298} = -74.8$ kJ/mol (15)

Here, at low temperature, all the CO and H_2 produced are consumed by reactions (12-15) with the consequent generation of methane and CO_2 as main gas products.

From Figure 1 it is evident that the hydrogen production rate and composition are strongly enhanced with the increase of temperature. Here, the higher the S/FUR, the higher the HY and $\%H_2$ concentration. The locus of maximum HR is located between 595-722°C, since there is a clear difference in HR from S/FUR = 8 (6.77) to 26 (9). Higher vales than S/FUR = 24, only increased the HR marginally, since S/FUR = 24 produced an HR of 8.9, while and S/FUR = 26 of 9. Also, it is important to notice that a greater amount of hydrogen is produced as the S/FUR increased towards relatively moderate lower temperatures. For example, in the case of the H_2 concentration plot (right), at S/FUR = 8 and 694°C a value of 57.3% H_2 is reached, while as S/FUR ratio increased to 25 and 586°C a value of 64.2% is achieved and this concentration remains almost constant forming a plateau for all S/FUR ratios as temperature increased above this point. This plateau in H_2 concentration can be explained in terms of the inhibition of the exothermic WGS reaction (19)

$CO(g) + H_2O(g) = CO_2(g) + H_2(g)$ $\Delta H°_{298} = -41.2$ kJ/mol (16)

Furthermore, at higher temperatures the CH_4 concentration decreases from 44% at 300°C to about 0.9% at 700°C for S/FUR = 8, while CO_2 concentration also decreases gradually from 48 to 17.4% at the same conditions. This can be seen at Figure 2 where the equilibrium compositions

for CH_4 and CO_2 are plotted. In general the trend observed in this Figure is that both methane and carbon dioxide are decreased as the reforming temperature is risen. Greater temperatures than 700°C will generate low levels of methane, while even at high S/FUR ratios CO_2 concentrations are as high as ≈ 30%. This behavior can be explained in terms that at high temperatures the furfural reforming reaction (9) is thermodynamically favored.

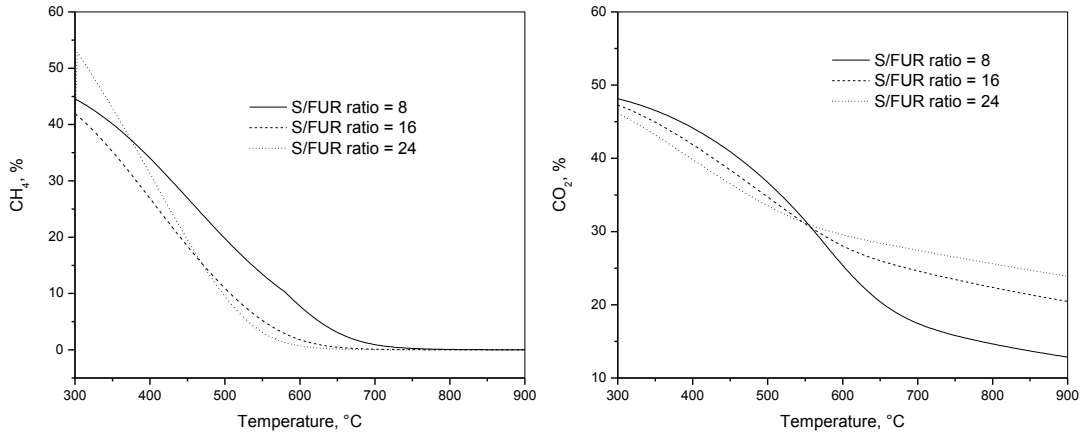

Figure 2. Equilibrium CH_4 and CO_2 Concentrations for Furfural Steam Reforming

At the same time, CO increase continuously from low to high temperatures from 0.05 to 29.5% from 300-850°C and S/FUR = 8. This behavior can be attributed to the reverse WGS reaction as can be seen in Figure 3, where the CO equilibrium concentration is plotted as a function of temperature and steam to furfural ratio.

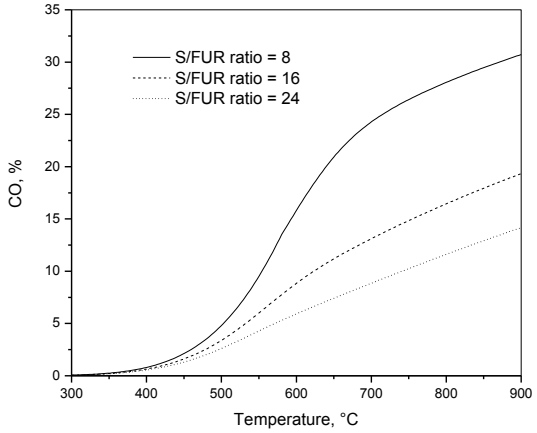

Figure 3. Equilibrium CO Concentrations for Furfural Steam Reforming

It is important to notice that CH_4 and CO_2 trend concentrations did not suffer mayor differences as the S/FUR changed, while steam feed content had a remarkable effect on the CO concentration as can be seen in results of Figure 3. The above described trends are consistent with previous thermodynamic analysis of bio oil system performed by Aktaş et al [33]. These authors claim that methane dry reforming (reverse reaction 12) and steam reforming (reverse reactions 13 and 14) domain at temperatures greater than 550°C. It is worth to mention that carbon formation was significant in this system at the stoichiometric ratio of S/FUR = 8. A more detailed analysis of the carbon generation will be presented in a separated section of the present study.

2.2.1 AESR of Furfural-CaO Absorbent

In the AESR using the CaO absorbent the hydrogen concentration is evidently enhanced as can be seen in Figure 4. The locus of maximum HR varies from 8 at 714°C and S/FUR = 8 to 9.94 at 596°C and S/FUR = 24, again here it can be seen a great difference in HR as the S/FUR increased from 8 to 9.94 of a maximum possible of 10, according to reaction (9). The difference observed in HR between S/FUR of 24 and 26 may be significant at temperatures greater than 650°C. However the desired operating reforming temperature implies lower temperatures. Therefore, an S/FUR of 24 will be enough to insure almost complete conversion of furfural to H_2 and to produce a 99.5% H_2 purity as long as the temperature is maintained below 600°C.

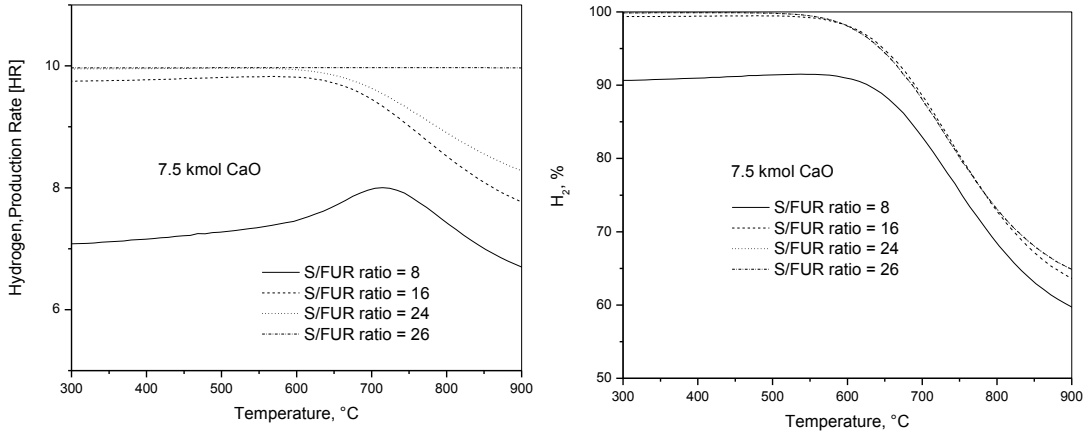

Figure 4. Equilibrium HR and H_2 for Furfural Steam Reforming using CaO as Absorbent

Also in Figure 4 the dry basis hydrogen concentration is plotted as a function of temperature and S/FUR ratio. Here it can be seen that an almost constant plateau in H_2 concentration is achieved at low temperatures (300-600°C) and this concentration is increased as the S/FUR also increase. The H_2 concentration at 550°C varied from 91.5% at S/FUR = 8 to 99.2% at S/FUR = 24. Greater temperature values than ≈ 600°C will eventually decrease the H_2% in the product gas. This can be attributed to the decrease of the ability of the CaO absorbent to capture CO_2 at high temperatures at the corresponding CO_2 partial pressure, since the carbonation reaction (1) is highly exothermic, which indicates that the CO_2 separation from the gas phase is inhibited at high temperatures. Also in this Figure it can be observed that S/FUR values greater than 24 do not represent a significant increase in HR as well as in %H_2 content at temperatures below 600°C. This means that a limit of S/FUR = 24 may play a significant role in determining if greater S/FUR values would represent an economical benefit (higher HR) compared to the cost of steam generation. Finally, the use of CaO as absorbent represented a 35.5% increase in hydrogen concentration with respect to furfural reforming without the use of a CO_2 absorbent.

Figure 5 presents CO_2 and CH_4 concentrations as a function of temperature and S/FUR ratio. Carbon dioxide concentrations are almost negligible at temperatures below 500°C. Greater temperature values resulted in increased CO_2 concentrations as high as 8.4% at 800°C and S/EtOH = 8, while at the same temperature an 18.1% CO_2 with S/EtOH = 24 can be achieved.

This behavior can be attributed to the fact that at low temperatures the ability of the CaO to capture CO_2 is enhanced due to the exothermic nature of the carbonation reaction. Also, at high temperatures, greater amounts of steam will promote the steam reforming reaction, thus producing more CO_2 susceptible of being carbonated. Also in Figure 5 it can be seen that the mayor contamination of the product gas at intermediate temperatures (300-600°C) is due to methane formation. Here in this plot the effect of the S/FUR on the CH_4 composition is evident, since at temperatures below 700°C the methanation reactions above described are favored for S/FUR ratio of 8, while higher ratios will eventually reduce methane concentrations at levels

below 0.11% at 500° and S/FUR = 24. This behavior can be explained by the enhancement of the steam reforming reaction at intermediate temperatures (300-600°C) by the use of a CO_2 absorbent, thus producing higher H_2 content and lower methane concentrations.

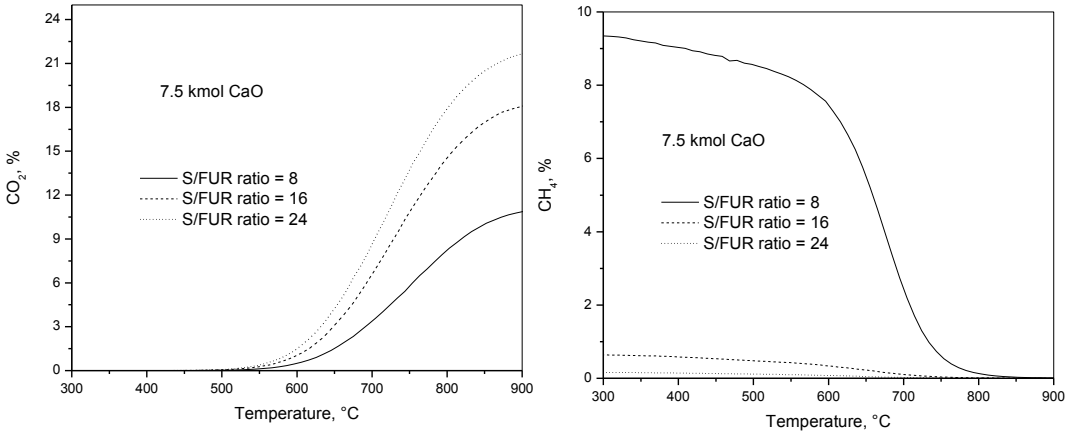

Figure 5. Equilibrium CO_2 and CH_4 compositions for Furfural Steam Reforming with CaO

Figure 6 shows the CO concentration as a function of S/FUR and temperature. In this Figure it can be seen that at temperatures below 500°C no CO is found and therefore the effect of the S/FUR is almost negligible, since there are no differences in CO composition at different steam contents.

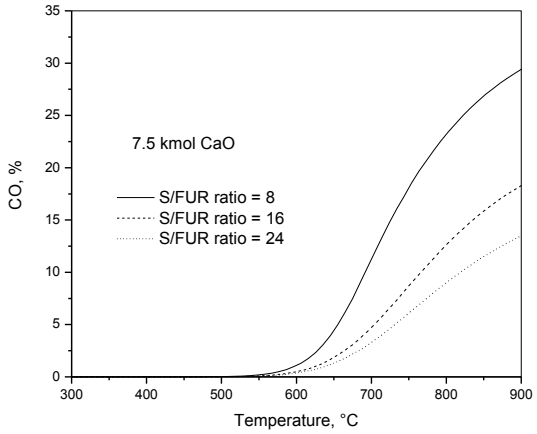

Figure 6. Equilibrium CO compositions for Furfural Steam Reforming with CaO

Also the effect of the CaO absorbent enhances the WGS and steam reforming reactions at temperatures lower than 550°C, thus avoiding a high CO content below this temperature. Higher temperatures than 550°C will increase the CO content in the product gas as the WGS would no longer be favored to react with steam.

*3.2.2 AESR of Furfural with CaO*MgO Absorbent*

Figure 7 presents the hydrogen production rate using calcined dolomite as a CO_2 absorbent in the steam reforming of furfural system. Here, it can be seen that there exist a locus of maximum hydrogen production as the S/FUR increases. For example, at S/FUR = 8 a HR of 8 is achieved at 724°C, while at S/FUR = 24 a HR of 9.9 can be produced at 586°C. These results are for practical purposes the same as with the use of CaO as absorbent. However, the durability of this mineral is several orders of magnitude greater than CaO and this dolomite can withstand as many as 15 carbonation/decarbonation cycles without mayor deterioration [34].

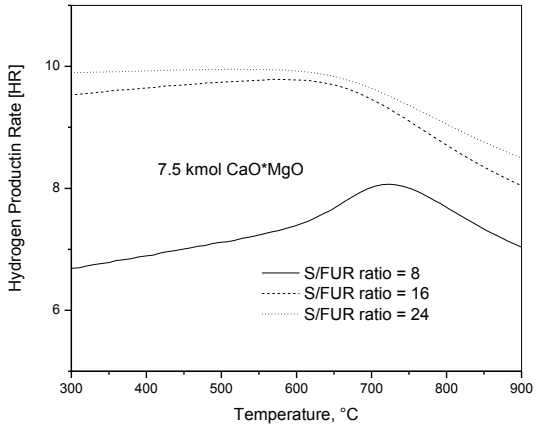

Figure 7. Equilibrium HR for Furfural Steam Reforming with CaO*MgO

Figure 8 shows a three dimensional scheme, where the all the gaseous species concentrations (%) are plotted as a function of temperature and S/FUR ratios.

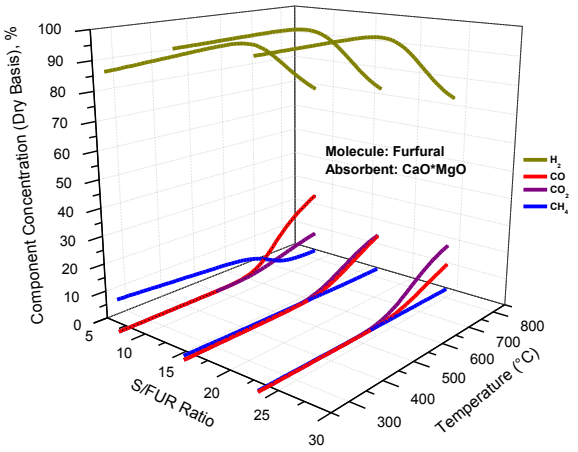

Figure 8. Equilibrium Compositions for Furfural Steam Reforming with CaO*MgO

In this plot it can be seen how the general trends for each gaseous species behave as a function of temperature and S/FUR ratio. For the case of hydrogen a concentration as high as 99.7% can be achieved at 517°C and S/FUR = 24. At low temperatures the hydrogen concentration remains high. For carbon oxides (CO and CO_2) both concentrations are small at low temperatures as a consequence of the CO_2 absorption enhancement effect of the dolomite and gradually increase as temperature is raised (S/FUR = 24,700°C) to values up to 8.9 and 11.5% for CO and CO_2, respectively. In Figure 8 it is evident that the mayor contaminant of the product gas is methane and this decreases as the temperature and S/FUR ratio increases, thus enhancing the steam reforming reaction.

3.2.3 AESR of Furfural with Na_2ZrO_3 Absorbent

Figure 9 presents the hydrogen production rate (HR) as a function of temperature and S/FUR ratio for the Na_2ZrO_3 absorbent. A maximum of HR of 9.8 can be obtained at 566°C and S/FUR of 24. The shapes of the curves resemble those observed for dolomite and CaO. However, the main difference is that at low temperatures (≈ 300°C) the product rate remains lower than that observed for CaO or dolomite. This behavior can be explained in terms of the different thermodynamic nature of the absorbents. For example, the Gibbs free energy of their carbonation reactions for CaO, CaO*MgO and Na_2ZrO_3 at 300°C are -87.12, -79 and -65.87 kJ/mol, respectively. While at high temperatures (≈ 650°C) this difference in Gibbs free energy is small

with values of -34.3, -25.8 and -24.6 kJ/mol, respectively. Therefore, the ability for the Na_2ZrO_3 to capture CO_2 at low temperatures is hindered by the nature of the absorbent. However, at high temperatures the absorbent is able to generate a HR quite comparable to those above reported for CaO and dolomite.

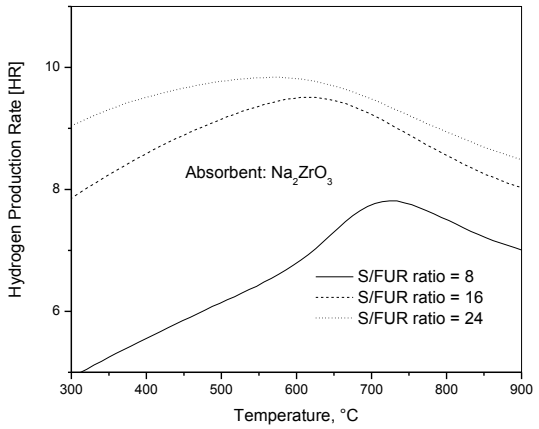

Figure 9. Equilibrium HR for Furfural Steam Reforming with Na_2ZrO_3

Figure 10 presents the equilibrium concentrations of H_2, CO, CO_2 and CH_4 as a function of temperature and S/FUR ratio for the Na_2ZrO_3 absorbent.

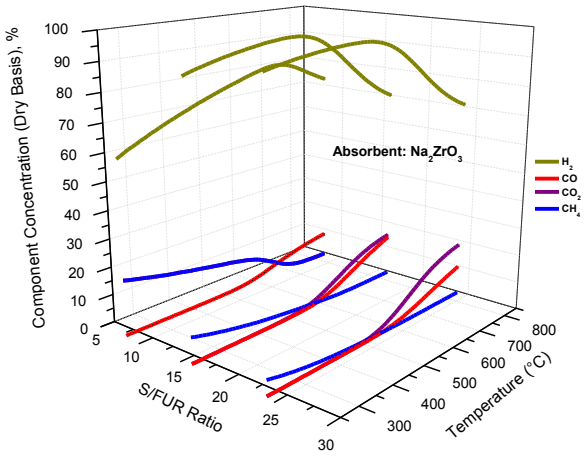

Figure 10. Equilibrium Compositions for Furfural Steam Reforming with Na_2ZrO_3

In this plot it can be seen that even at low temperatures the hydrogen concentrations remain high (> 90% H_2 for S/FUR ratios ≥ 16) and eventually peak to a maximum of 99% H_2 at 500°C and S/FUR = 24. Greater temperatures than 600°C will produce, as in previous absorbents (CaO and CaO*MgO), a gradual decrease of the hydrogen content in the gas product. The production of carbon oxides at low temperatures are somewhat a little higher than with previous absorbents because of the behavior above described.

3.2.4 AESR of Furfural with Li_2ZrO_3 Absorbent

Results for the steam reforming of furfural using Li_2ZrO_3 as CO_2 absorbent were very similar to those presented for Na_2ZrO_3. In fact, the shape of the HR as a function of temperature and S/FUR was the same. Only slight differences appeared since a maximum HR of 9.82 can be obtained at 576°C and S/FUR of 24. Otherwise, the trends and shapes for all gaseous species in the product gas were essentially the same, with a maximum H_2 concentration of 99% at 468°C and S/FUR of 24. All these similarities can be explained in terms of the thermodynamic nature of these absorbents. A comparison in terms of the Gibbs free energy of the carbonation reactions (5) and (6) at 600°C results in very small differences since Na_2ZrO_3 and Li_2ZrO_3 exhibit values of -24.58 and -23.53 kJ/mol, respectively.

3.2.5 AESR of Furfural with Li_4SiO_4 Absorbent

Figure 11 shows the hydrogen production rate (HR) as a function of temperature and S/FUR ratio for the Li_4SiO_4 absorbent. Here it can be observed that a maximum of HR of 9.5 can be obtained at 596°C and S/FUR of 24.

The shape of the HR curves appeared to be different compared to the ones observed for Na_2ZrO_3 and Li_2ZrO_3, especially in the range of 300-500°C, where lower HR values are observed. This behavior reflects the fact that the hydrogen production is somewhat limited by the absorption ability of Li_4SiO_4 to capture CO_2, especially at low temperatures (≈ 300°C). This is more evident when a comparison is made between the curves for S/FUR ratios 8 and 16.

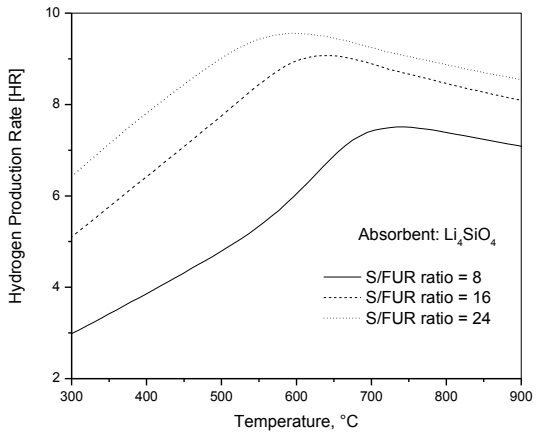

Figure 11. Equilibrium HR for Furfural Steam Reforming with Li_4SiO_4

Figure 12 shows the equilibrium concentrations of H_2, CO, CO_2 and CH_4 as a function of temperature and S/FUR ratio for the Li_4SiO_4 absorbent.

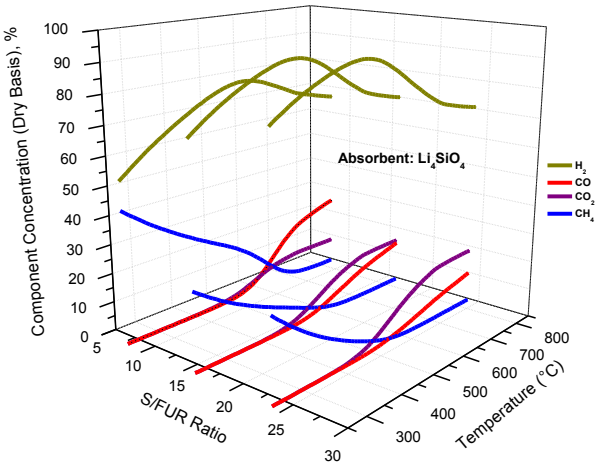

Figure 12. Equilibrium Compositions for Furfural Steam Reforming with Na_2ZrO_3

According to results from Figure 12 it can be seen that the trends and shapes of all gaseous species in the product gas were similar to those presented for the zirconates. However, the values for hydrogen concentrations were lower accompanied with higher values of methane, especially

at low temperatures. This was reflected in the maximum H_2 concentration which was 94.5% at 468°C and S/FUR of 24.

3.2.6 Absorbent Comparison for Furfural Reforming

Table 1 presents a summary of simulation results for the steam reforming of furfural with and without the use of a CO_2 absorbent. Conditions reported in this table were close to the maximum hydrogen production obtained for each absorbent and these were; S/FUR = 24:1 and at 550°C. This temperature was chosen because it represents the average of the maximum hydrogen production in all performed calculations. This Table shows the evident limitation of the steam reforming of ethanol (SR) without absorbent, since only 8.3 mols of H_2 were produced per mol of furfural. Even at this relatively moderate temperature the amounts of CO, CH_4 and CO_2 are relatively high, with 0.56, 4.16 and 0.288 mols at equilibrium, respectively. Also the hydrogen concentration was only of 62.4%. The expected enhancement with the use of a CO_2 absorbent is clear when a comparison is made with respect to the values obtained for CaO. In Table 1 the increase in hydrogen production was of 16.2% greater with the use of CaO. Consequently, the other gaseous species were reduced. CO produced was reduced 93 times, while CO_2 was reduced 138 times. Also, methane was reduced 36 times. All this is translated in a very high hydrogen concentration which for this absorbent reached 99.5%.

Table 1. Summary of Simulation Results for Furfural Steam Reforming at 550°C

Absorbent	Mols at Equilibrium				Parameters	
	H_2	CO	CO_2	CH_4	S/FUR ratio	$\%H_2$
CaO	9.9	0.006	0.03	0.008	24:1	99.5
CaO*MgO	9.9	0.008	0.05	0.01	24:1	99.3
Na_2ZrO_3	9.8	0.029	0.17	0.036	24:1	97.6
Li_2ZrO_3	9.8	0.03	0.18	0.038	24:1	97.5
Li_4SiO_4	9.4	0.114	0.72	0.119	24:1	90.8
No Absorbent	8.3	0.56	4.16	0.288	24:1	62.4

Other absorbents behaved similarly to the results presented in the previous section. For example, calcined dolomite (CaO*MgO) exhibited only a small difference in results with respect to CaO. Since, the hydrogen production was the same, while CO and CO_2 were increased 33 and 66% from the values produced using CaO. However, these values were 16% higher in H_2 production and 37% in hydrogen concentration (99.3%) compared with conventional SR (62.4%). Results for the zirconate absorbents Na_2ZrO_3 and Li_2ZrO_3 were very similar between them and to the ones for CaO*MgO as can be seen in Table 1. For example, hydrogen production for Na_2ZrO_3 and Li_2ZrO_3 were the same with 9.8 compared to 9.9 for CaO*MgO. Equilibrium mols of CO followed the same trend, while CO_2 mols presented only a slight decrease of the zirconate absorbents compared to those produced by calcined dolomite (0.05 compared to 0.17 and 0.18) and the same trend occurred with methane formation. However, hydrogen concentration was just slightly less for the zirconates (97%) compared to the concentration produced by calcined dolomite (99%).

Li_4SiO_4 was the absorbent that produced the lowest hydrogen production and higher by product concentrations (CO, CO_2 and CH_4). This was translated in a lower hydrogen concentration of only 90.8%. This behavior can be attributed to the thermodynamic nature of this absorbent. For example, if the Gibbs free energy of carbonation at 550°C is compared between the zirconates and the lithium orthosilicate, there exists a significant difference with values of -31.3 and -30.7 kJ/mol for Na_2ZrO_3 and Li_2ZrO_3, respectively to a value of -18.3 kJ/mol for Li_4SiO_4.

Therefore, a crucial feature within the hydrogen production through the absorption enhanced steam reforming (AESR) of bio-oil model compounds resides in nature of the CO_2 solid absorbent, which apart from favorable thermodynamics, must present adequate absorption capacity and fast absorption-regeneration kinetics. Several researches have focused their studies in the effects of pressure, temperature and gas reactant composition on absorbents based on calcium oxide (CaO) using the thermogravimetric (TGA) experimental technique [35, 36]. However, sintering of these materials reduce their performance after several absorption-

regeneration cycles. Calcined dolomite (CaO*MgO) have shown to better perform in CO_2 absorption at high temperatures compared to CaO in multicycle tests [36]. Unfortunately, this mineral origin absorbent requires high regeneration temperatures (T ≥ 950 °C) that produce degradation of the material after 10 absorption-regeneration cycles. Bandi et al. [37] proposed the use of the mineral huntite ($Mg_3Ca(CO_3)_4$) exhibiting good regeneration performance. However, this absorbent has several disadvantages such as: a high regeneration temperature and low CO_2 capacity. Also of mineral origin the $Mg_6Al_2(CO_3)(OH)_{16}*4H_2O$ hydrotalcite was proposed by Hufton et al. [7] and Ding and Alpay [38] which used this CO_2 adsorbent at moderate temperatures (400-500 °C) resulting in low adsorption capacity.

Studies by López Ortiz et al., [13] have shown the superior performance of Na_2ZrO_3 as an alternate synthetic CO_2 solid absorbent compared to expensive lithium-base absorbents (Li_2ZrO_3 and Li_4SiO_4, Nakagawa and Ohashi [39] and Kato et al, [40]). This behavior was attributed on its excellent thermal stability, kinetics and CO_2 capture capacity features.

Recently, Ochoa Fernandez et al., [41] have experimentally evaluated several synthetic CO_2 absorbents, under the AESR of methane reaction scheme, such as: Li_2ZrO_3, Li_4SiO_4 and Na_2ZrO_3 and concluded that Na_2ZrO_3 is the one that better performed towards high methane conversions, hydrogen purity and reaction kinetics. Furthermore, Jakobsen and Halmøy [42] performed a reactor modeling of the sorption enhanced steam methane reforming using CaO, Li_4SiO_4 and Na_2ZrO_3 and also concluded that Na_2ZrO_3 is the most efficient absorbent with the highest hydrogen production rate (92.6%) compared to CaO (79.3%) and Li_4SiO_4 (82.1%) at the same reaction conditions in a temperature range from 600°C to 800°C.

Therefore, from the above presented thermodynamic analysis of the absorption enhanced for furfural model compound reforming it can be concluded that Na_2ZrO_3 is a promising alternate absorbent with comparable thermodynamics and greater kinetics and stability.

3.3 DMP Steam Reforming System

3.3.1 DMP AESR Gas Product Distribution without Absorbent

Figure 13 shows the equilibrium hydrogen production rate (HR) and H_2 concentration (%) as a function of temperature (300-800°C) and S/DMP ratio (15-45). In this Figure it can be seen that a maximum of 14.4 HR was reached at 743°C and S/DMP of 15 (stoichiometric condition according to equation 10). As the S/DMP ratio is increased from 15 to 45 the HR also raised towards values located at lower temperatures. For example, a maximum of 18.1 HR was achieved at 635°C and S/DMP of 45.

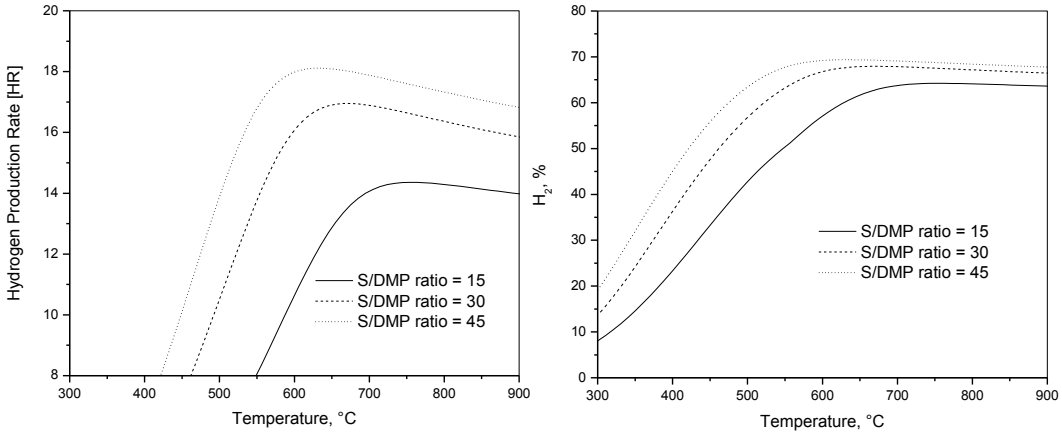

Figure 13. Equilibrium HR and H_2 for DMP Steam Reforming

This behavior, as in the case for the furfural reforming, can be explained by the promotion of the methanation reactions at low temperatures (300-500°C). Otherwise, at stoichiometric conditions (S/DMP = 15), a maximum hydrogen concentration of 64% was reached at 724°C. Again, the increase in S/DMP ratio resulted in higher hydrogen concentrations towards lower temperatures. Since a value of 69% was reached at 653°C and S/DMP of 45.

Figure 14 portrays the carbon oxide equilibrium compositions for DMP reforming. In this Figure it can be seen that CO is produced at relatively small concentrations at low temperatures (300-500°C) and as temperature increases CO concentrations also is raised and can be as high as 21.7%

at 700°C and S/DMP ratio of 45. CO production at high temperature is generated through the dry reforming and steam reforming reactions, reverse reactions (12) and (13), respectively. This is the reason why the CO concentration is increased at high temperatures than 500°C, while CO_2 and CH_4 concentrations are reduced in this particular region.

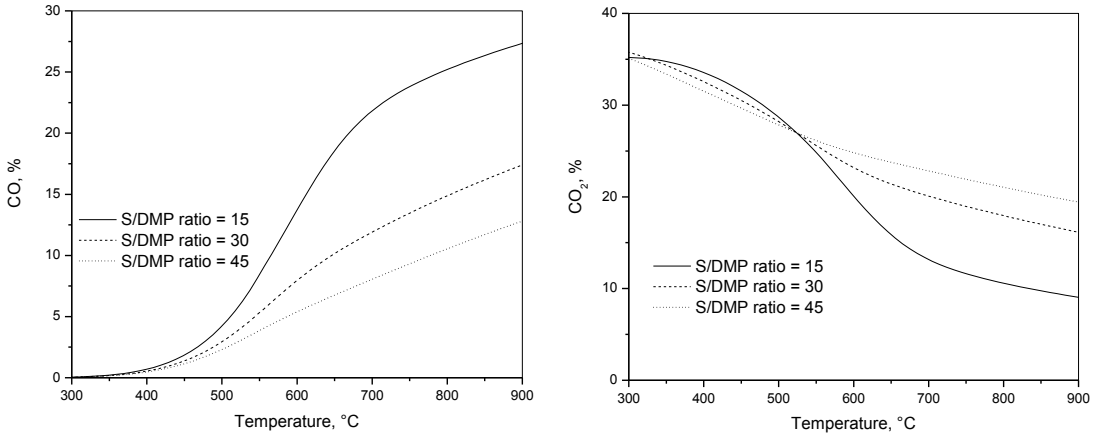

Figure 14. Equilibrium CO and CO_2 Compositions for DMP Steam Reforming

Furthermore, the CO_2 concentration is high at relatively low temperatures (300-500°C). This is due to the methanation reaction (12), which favors the production of CO_2 and methane at low temperatures. Similarly, as temperature is increased CO_2 is reduced due to the dry reforming reaction (reverse reaction 12) and to the fact that the WGS reaction is no longer favorable at these conditions.

Figure 15 presents the methane concentration profile as a function of temperature and S/DMP ratio. In this plot it can be seen, as pointed out above, that methane concentrations at low temperatures are high due to the promotion of the methanation reactions (12-15). Also, as temperature increases these concentrations are reduced due to the promotion of the steam and dry methane reforming reactions. The effect of the S/DMP ratio on the reduction of methane content is also evident in this plot especially in the range of 300-500°C. A greater content of steam would eventually have positive effect on the methane steam reforming reaction and hence reduce the methane content as the S/DMP ratio is increased.

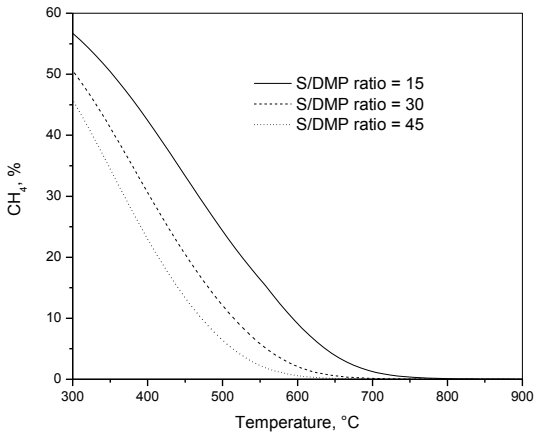

Figure 15. Equilibrium CH_4 Compositions for DMP Steam Reforming.

Furthermore, as temperature increases this behavior is magnified particularly at temperatures higher than 500°C. This behavior again, is consistent with the fact that a higher steam concentration will favor the steam methane reforming reaction towards a higher production of H_2 and CO_2.

3.3.2 DMP Reforming Gas Product Distribution

Figure 16 shows results of the steam reforming of DMP. In this Figure equilibrium concentrations for gaseous species H_2, CO, CO_2 and CH_4 are plotted as a function of temperature and S/DMP ratio. In this Figure it is evident the complex composition of the gas product, especially at temperatures lower than 500°C, where a mixture of methane, carbon dioxide and hydrogen are the predominant species in the gas product. Also, it can be seen that the effect of S/DMP ratio is not that significant. For the entire range studied. However this effect become important as temperature is increase above 500°C.

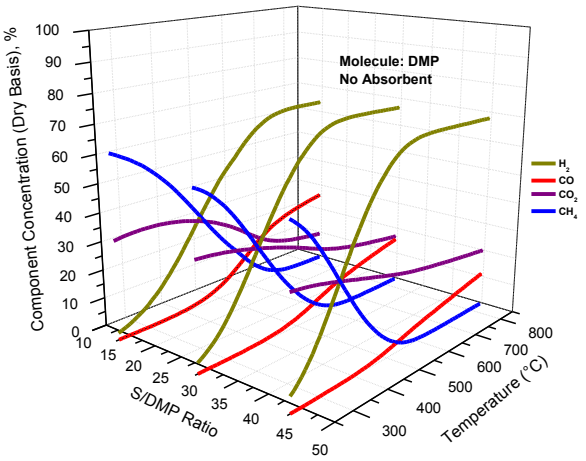

Figure 16. Equilibrium Compositions for DMP Steam Reforming

3.3.3 DMP Reforming Gas Product Distribution with CaO as CO_2 Absorbent

Figure 17 shows a three dimensional scheme, where the all the gaseous species concentrations (%) are plotted as a function of temperature and S/DMP ratios for the steam reforming of methanol with CaO as a CO_2 absorbent.

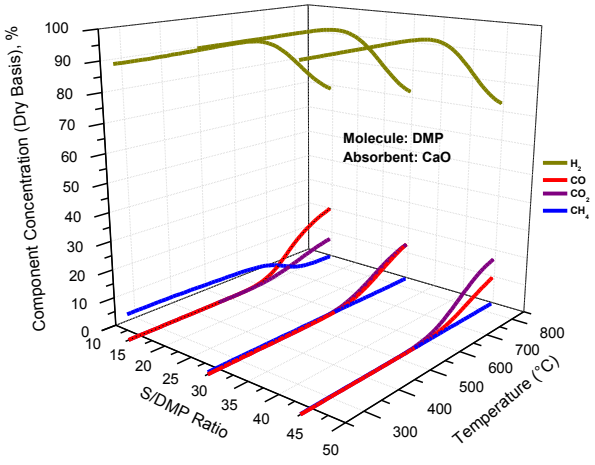

Figure 17. Equilibrium Compositions for DMP Steam Reforming with CaO.

In this plot it can be seen how the general trends for each gaseous species behave as a function of temperature and S/DMP ratio. For the case of hydrogen a concentration as high as 99.8% can be

achieved at 500°C and S/DMP = 45. It is important to mention that the concentration that is obtained at these conditions is not that different compared to the one that can be obtained at a lower S/DMP ratio of 30, since the H_2 concentration at this ratio is 99.4%, which represents a negligible difference. Also the amount of HR using S/DMP ratios of 30 and 45 is very close with values of 19.9 and 19.6, respectively. Therefore it can be inferred that a S/DMP ratio of 30 would be high enough to obtain a very high hydrogen content in the product gas.

Also in Figure 17 it can be seen that at low temperatures the hydrogen concentration remains high, even for the case of the stoichiometric value (92% H_2 at 556°C, S/DMP = 15). For carbon oxides (CO and CO_2) both concentrations are very small at low temperatures as a result of the CO_2 absorption enhancement effect of CaO and gradually increased as temperature was raised (T > 500°C) to values up to 12.2 and 3.10% for CO and CO_2 (S/DMP = 15 and 700°C), respectively. A comparison of this plot and Figure 16 (DMP, no absorbent) makes evident the great improvement that the AESR reaction scheme has on the hydrogen production and purity of the gas product, especially at temperatures below 600°C.

In Figure 17 it is clear that the only significant contaminant of the product gas at low temperatures is methane. This is decreased as the temperature and S/MeOH ratio also increased, thus enhancing the steam reforming reaction. Greater values of S/DMP = 15 will insure very low CH_4 concentrations (less than 1%) in the temperature range of 300-600°C.

*3.3.4 DMP Reforming Gas Product Distribution with CaO*MgO as CO_2 Absorbent*

Figure 18 shows the equilibrium concentrations of H_2, CO, CO_2 and CH_4 as a function of temperature and S/DMP ratio for the CaO*MgO absorbent. In this plot it can be seen that the concentration profiles of each species generated with the CaO*MgO absorbent are very similar to the ones produced for CaO. The only apparent difference is the slightly higher levels of methane formation at low temperatures (300-500°C) and specifically at S/MeOH = 15 (stoichiometric conditions).

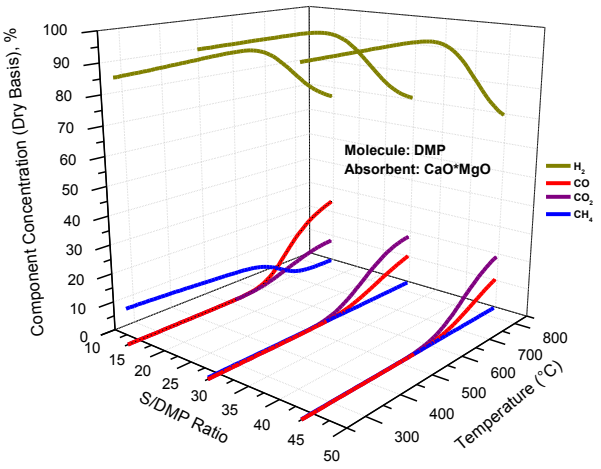

Figure 18. Equilibrium Compositions for DMP Steam Reforming with CaO*MgO

3.3.5 DMP Reforming Gas Product Distribution with Na_2ZrO_3 as CO_2 Absorbent

Figure 19 shows results of the steam reforming of DMP using Na_2ZrO_3 as a CO_2 absorbent. In this Figure equilibrium concentrations for gaseous species H_2, CO, CO_2 and CH_4 are plotted as a function of temperature and S/DMP ratio.

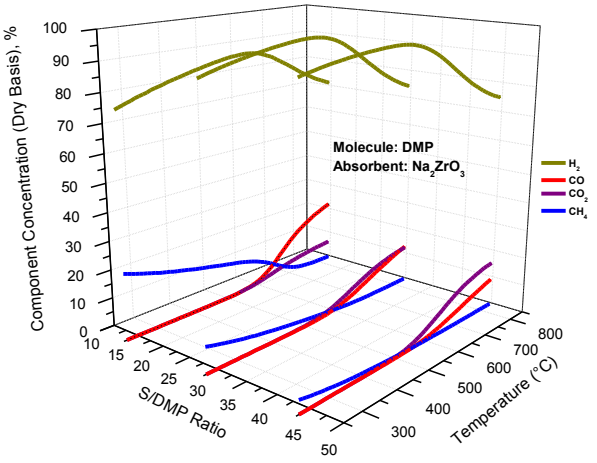

Figure 19. Equilibrium Compositions for DMP Steam Reforming with Na_2ZrO_3

In this Figure it can be seen that even at low temperatures the hydrogen concentrations remains high (> 80% H_2) and eventually peak to a maximum of 98.4% H_2 at 468°C and S/DMP = 45. A

smaller S/DMP ratio of 30 only changes this concentration to a value of 97.2% at 507°C. Greater temperatures than 600°C will produce as in previous absorbents (CaO and CaO*MgO) a gradual decrease of the hydrogen content in the product gas. A slightly higher production of carbon oxides than with the use of calcium absorbents is observed at high temperatures with values as high as 13 and 4.3% for CO and CO_2, respectively (T= 700°C and S/DMP = 15). This behavior is associated with the thermodynamic nature of the CaO absorbent, which absorption Gibbs free energy at 550°C is 1.69 times more negative than for the Na-based absorbent (Na_2ZrO_3).

3.3.6 DMP Reforming Gas Product Distribution with Li_2ZrO_3 as CO_2 Absorbent

Figure 20 presents a three dimensional plot where results of the steam reforming of DMP equilibrium concentrations using Li_2ZrO_3 as a CO_2 absorbent are presented as a function of temperature and S/DMP ratio.

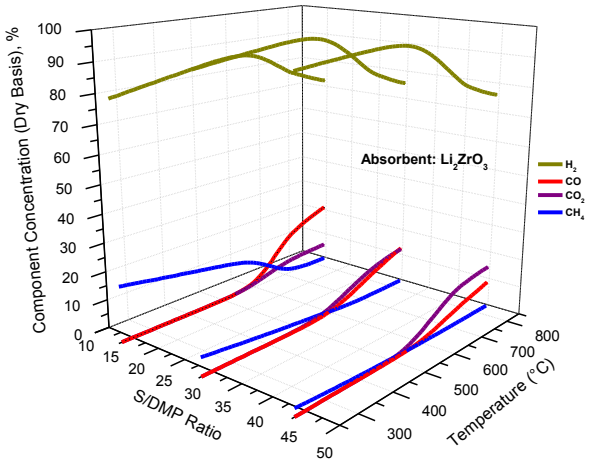

Figure 20. Equilibrium Compositions for DMP Steam Reforming with Li_2ZrO_3

\Results from Figure 20 using Li_2ZrO_3 make evident that the trends and equilibrium concentrations are almost the same as with Na_2ZrO_3. However, there is a slight difference mainly in the methane concentration at low temperatures, which for the Li-based absorbent is slightly smaller than that observed for Na_2ZrO_3 in Figure 19. For example for Na_2ZrO_3 a value of 19.6% CH_4 was generated at 300°C and S/DMP ratio of 15 (stoichiometric condition), while a value of

17.5 was generated by Li_2ZrO_3. Other than that results were essentially the same between zirconate absorbents.

3.3.7 DMP Reforming Gas Product Distribution with Li_4SiO_4 as CO_2 Absorbent

Figure 21 shows the equilibrium concentrations of H_2, CO, CO_2 and CH_4 as a function of temperature and S/MeOH ratio for the Li_4SiO_4 absorbent.

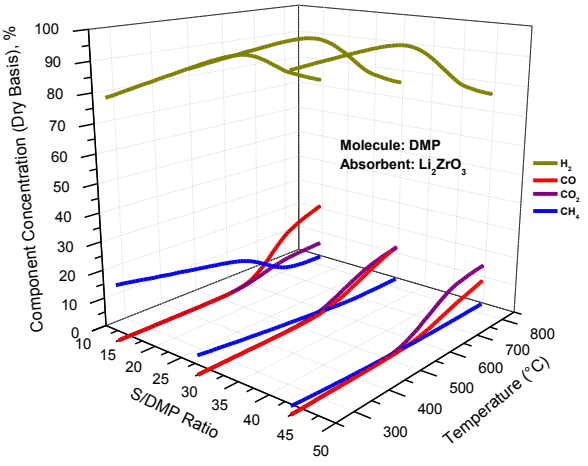

Figure 21. Equilibrium Compositions for DMP Steam Reforming with Li_2ZrO_3

Results from Figure 21 indicate that the trends and shapes of all gaseous species in the product gas were similar to those presented for the zirconates. However, the values for hydrogen concentrations were lower and accompanied with higher values of methane, especially at low temperatures. This was reflected in the maximum H_2 concentration which was 94.5% at 468°C and S/DMP of 45.

3.3.8 Absorbent Comparison for DMP Reforming

Table 2 shows a summary of simulation results for the steam reforming of DMP with and without the use of a CO_2 absorbent. Conditions reported in this table were close to the maximum hydrogen production obtained for each absorbent and these were; S/DMP = 45:1 and at 500°C. This temperature was chosen because it represents the average of the maximum hydrogen

production in all performed calculations. This Table shows the evident limitation of the steam reforming of DMP without absorbent, since only 13.7 mols of H_2 were produced per mol of DMP. Even at this moderate high temperature the amounts of CO, CO_2 and CH_4, are relatively high with 0.480, 6.06 and 1.44 mols at equilibrium, respectively. Also, the hydrogen concentration was only of 63.2%. The expected enhancement with the use of a CaO absorbent was very significant, since a comparison between this with respect to DMP steam reforming without the use of an absorbent represents an increase of 45.2% in hydrogen production. However, the main difference is achieved in the byproduct gaseous concentrations, which all were significantly reduced. Using CaO, CO produced was reduced 282 times, while CO_2 was reduced 466 times. Also, methane was reduced 68.6 times. All this was translated in a very high hydrogen concentration, which for this absorbent was 99.1%, an increase of about 36% with respect to DMP reforming without absorbent.

Table 2. Summary of Simulation Results for DMP Steam Reforming at 500°C

Absorbent	Mols at Equilibrium				Parameters	
	H_2	CO	CO_2	CH_4	S/DMP ratio	$\%H_2$
CaO	19.9	0.002	0.013	0.021	45:1	99.1
CaO*MgO	19.8	0.004	0.035	0.053	45:1	99.5
Na_2ZrO_3	19.5	0.011	0.091	0.130	45:1	98.8
Li_2ZrO_3	19.5	0.011	0.092	0.131	45:1	98.8
Li_4SiO_4	17.9	0.060	0.540	0.517	45:1	93.7
No Absorbent	13.7	0.480	6.060	1.440	45:1	63.2

Other absorbents behaved similarly to the results presented in the previous section. For example, calcined dolomite (CaO*MgO) exhibited only a small difference in results with respect to CaO. Here, the hydrogen production was practically the same (19.8 and 19.9), while CO and CO_2 were almost doubled from the values produced using CaO. Nevertheless, these values were essentially the same in terms of hydrogen concentration (99%), while this represented an increase of 36% with respect to conventional DMP steam reforming (63%). As with the previous molecule (FUR), results for the zirconate absorbents Na_2ZrO_3 and Li_2ZrO_3 were very similar between them and to

the ones for CaO*MO as can be seen in Table 2. For instance, hydrogen production rate (HR) for Na_2ZrO_3 and Li_2ZrO_3 were both 19.5 mols at equilibrium compared to 19.8 for CaO*MgO. Equilibrium mols of CO followed the same trend, while CO_2 mols presented only a slight increase of the zirconate absorbents compared to those produced by calcined dolomite (0.035 compared to 0.091 and 0.092) and the same trend occurred with methane formation. However, hydrogen concentration was just slightly smaller than that for the zirconates Na_2ZrO_3 (98.8%) compared to the concentration produced by calcined dolomite (99.5%).

Similarly to the case for furfural reforming, DMP reforming using Li_4SiO_4 produced the lowest hydrogen production and higher byproduct concentrations (CO, CO_2 and CH_4). This was translated in a lower hydrogen concentration of only 93.7%. This behavior can be attributed to the limited thermodynamic nature of this absorbent as referenced before in the furfural reforming section.

3.4 VAI Steam Reforming System

3.4.1 VAI AESR Gas Product Distribution without Absorbent

Figure 22 shows the equilibrium hydrogen production rate (HR) and H_2 concentration (%) as a function of temperature (300-800°C) and S/VAI ratio (13-39). In this Figure it can be seen that a maximum of 11.7 HR was reached at 737°C and S/VAI of 13 (stoichiometric condition according to equation 11). Again, as the S/VAI ratio is increased from 13 to 39 the HR also was risen towards values located at lower temperatures. For example, a maximum of 15.2 HR was achieved at 626°C and S/DMP of 39.

At stoichiometric conditions (S/VAI = 13), a maximum hydrogen concentration of 59.4% was reached at 737°C. Again, the increase in S/VAI ratio resulted in higher hydrogen concentrations towards lower temperatures. Since a value of 64.9% was reached at 575°C and S/VAI of 39. It is worth mentioning that these temperatures are very similar compared to the results observed for furfural. In fact, maximum hydrogen content was achieved for VAI ($C_8H_8O_3$), FUR ($C_5H_4O_2$) and

DMP ($C_8H_{10}O$) at temperatures 686, 688 and 753°C. This behavior is consistent with results obtained by Lima da Silva and Müller [43] who compared several oxygenated hydrocarbons under the AESR reaction scheme and found the following behavior; the higher the oxygen content (in the hydrocarbon), the lower the maximum hydrogen temperature and related this with a higher oxidative environment within the reaction system.

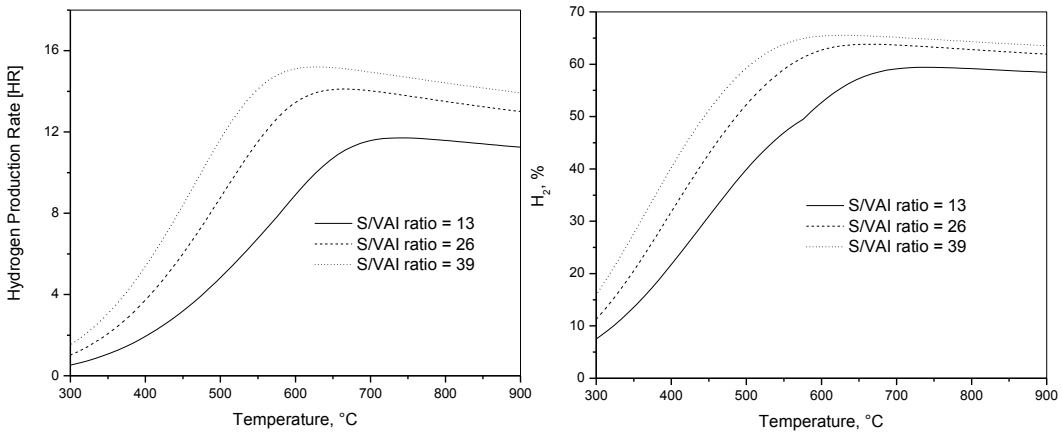

Figure 22. Equilibrium HR and H_2 for VAI Steam Reforming.

Figure 23 presents the carbon oxide equilibrium compositions for VAI reforming. In this Figure it can be seen that CO is produced at relatively small concentrations at low temperatures (300-500°C) and as temperature increases CO concentrations also is raised and can be as high as 24% at 700°C and S/VAI ratio of 13 (stoichiometric ratio).

Furthermore, the CO_2 concentration is high at relatively low temperatures (300-500°C), and in this region the S/VAI ratio do not seem to present a significant effect.

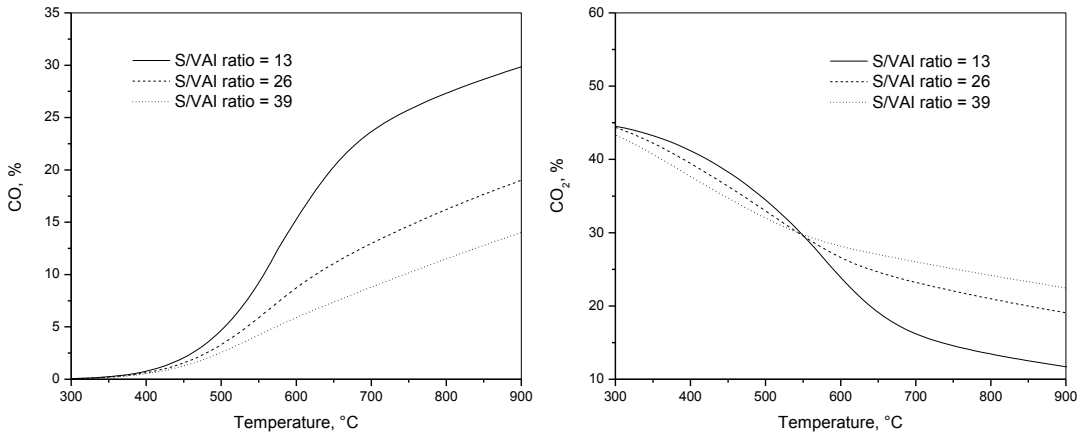

Figure 23. Equilibrium CO and CO_2 Compositions for VAI Steam Reforming

Figure 24 presents the methane concentration profile as a function of temperature and S/VAI ratio. In this plot it can be seen, as pointed out above, that methane concentrations at low temperatures are high due to the promotion of the methanation reactions. Also, conversely as temperature increases carbon dioxide and methane are reduced due to the enhancement of the steam and dry methane reforming reactions.

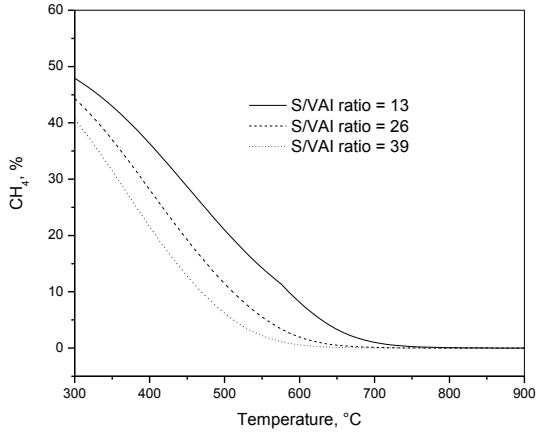

Figure 24. Equilibrium CH_4 Compositions for DMP Steam Reforming.

Furthermore, greater temperatures than 500°C will reduce the methane content in the product gas.

3.4.2 VAI Reforming Gas Product Distribution

Figure 25 shows results of the steam reforming of VAI. In this Figure equilibrium concentrations for gaseous species are presented as a function of temperature and S/VAI ratio.

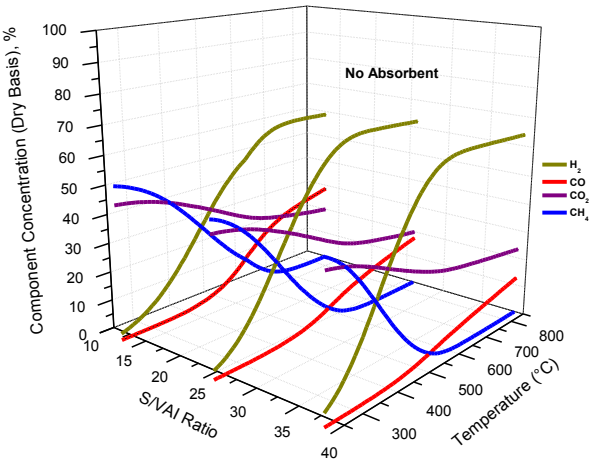

Figure 25. Equilibrium Compositions for VAI Steam Reforming

In this Figure it is evident the content of by-product contaminants (CO, CO_2 and CH_4) in the product gas, especially at temperatures lower than 500°C. Also, it can be seen that the effect of S/VAI ratio is not significant. Since the variation in concentrations as this ratio varied was not important. Therefore, it can be concluded that in this system the hydrogen production is thermodynamically limited for the S/VAI ratios and temperatures studied.

3.4.3 VAI Reforming Gas Product Distribution with Using CO_2 Absorbents

Figure 26 presents a three dimensional graph, where the all the gaseous species concentrations (%) are plotted as a function of temperature and S/VAI ratios for the steam reforming of vanillin with CaO as a CO_2 absorbent.

Here, the general trends for each gaseous species behave very similar as with the other FUR and DMP previously presented and a hydrogen a concentration as high as 99.9% can be achieved at 429°C and S/VAI = 39. Also the amount of HR using S/VAI = 6.9 is practically the same for the theoretical maximum conversion to hydrogen, which is 17. A lower S/VAI 26 results in a HR

value of 16.7. Therefore it can be concluded that S/VAI ratio of 26 would be high enough to obtain very high hydrogen content in the product gas.

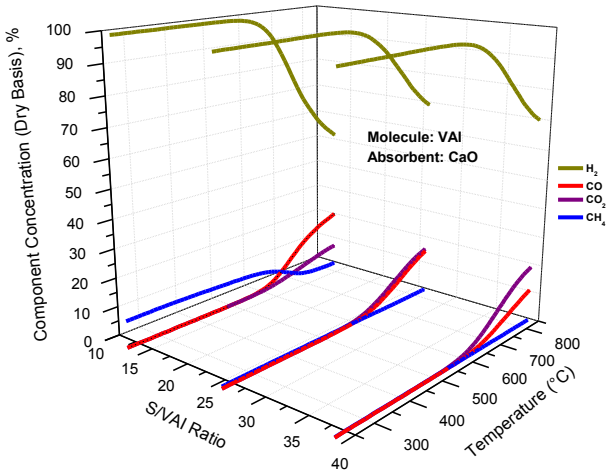

Figure 26. Equilibrium Compositions for DMP Steam Reforming with CaO

The use of other absorbent such as CaO*MgO, Na_2ZrO_3, Li_2ZrO_3 and Li_4SiO_4 presented almost the same behavior as the other model molecules (FUR and DMP). Figure 27 presents a set of four images where the product distributions of all these absorbents are presented as a function of temperature and S/VAI ratio.

Most of the gas species appear in very similar trends as the previous DMP model molecule. Results of maximum hydrogen concentrations and its related temperature are presented in Table 3 for every single absorbent used in the thermodynamic modeling of the VAI reforming system at a S/VAI ratio of 39.

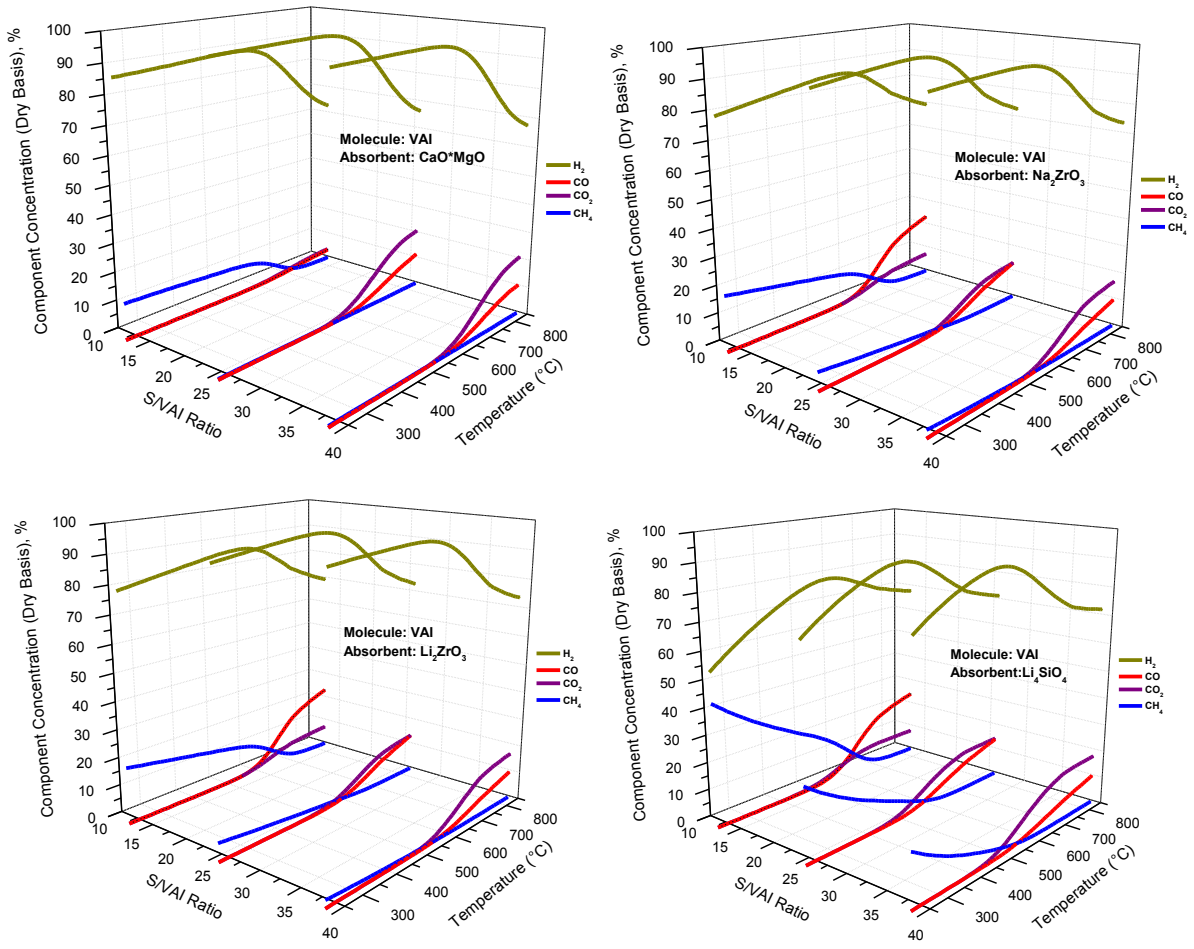

Figure 27. VAI AERS Compositions with CaO*MgO, Na_2ZrO_3, Li_2ZrO_3 and Li_4SiO_4 Absorbents

Table 3. Maximum Hydrogen Concentration and Related Temperature for the AESR of VAI

Absorbent	Maximum H_2, %	Temperature, °C
CaO	99.9	429
CaO*MgO	99.7	439
Na_2ZrO_3	99.0	468
Li_2ZrO_3	99.0	448
Li_4SiO_4	94.4	468

Here in this table it can be seen that very high concentrations can be achieved with the AESR of VAI. Temperatures for most absorbents ranged from 429°C for CaO to 468°C for Li_4SiO_4. Therefore, 450°C is an average temperature where the maximum hydrogen content occurs for all absorbents in AESR of vanillin.

3.4.4 Absorbent Comparison for VAI Reforming

Table 4 shows a summary of simulation results for the steam reforming of VAI with and without the use of a CO_2 absorbent. Conditions reported in this Table were close to the maximum hydrogen production obtained for each absorbent and these were; S/VAI = 39:1 and at 450°C. This Table shows the evident limitation of the steam reforming of VAI without absorbent, since only 8. mols of H_2 were produced per mol of VAI. Level concentrations of CO, CO_2 and CH_4, were high with 0.187, 5.62 and 2.19 mols at equilibrium, respectively. Also, the hydrogen concentration was only of 57.2%. The expected enhancement with the use of a CaO absorbent was very significant, since a comparison between this (16.9) with respect to VAI steam reforming without the use of an absorbent (8) represents an increase of 111% in hydrogen production. However, the main difference is achieved in the byproduct gaseous concentrations, where all were significantly reduced. Using CaO, CO produced was reduced 282 times, while CO_2 was reduced 466 times. Also, methane was reduced 1246 times. All this was translated in a very high hydrogen concentration, which for this absorbent was 99.9%, an increase of about 42% with respect to VAI reforming without absorbent.

Table 4. Summary of Simulation Results for VAI Steam Reforming at 450°C

Absorbent	Mols at Equilibrium				Parameters	
	H_2	CO	CO_2	CH_4	S/VAI ratio	$\%H_2$
CaO	16.9	0.00015	0.00018	0.019	39:1	99.9
CaO*MgO	16.8	0.00040	0.0050	0.050	39:1	99.7
Na_2ZrO_3	16.4	0.00133	0.0163	0.148	39:1	99.0
Li_2ZrO_3	15.1	0.00138	0.0097	0.475	39:1	99.0
Li_4SiO_4	14.2	0.09890	0.1460	0.698	39:1	94.4
No Absorbent	8.0	0.18700	5.6200	2.190	39:1	57.2

Other absorbents behaved similarly to the results presented in the previous section. For example, calcined dolomite (CaO*MgO) exhibited virtually the same results with respect to CaO. While CO and CO_2 were almost doubled from the values produced using CaO. However, these values were essentially the same in terms of hydrogen concentration (99%), while this represented an increase of 42% with respect to conventional DMP steam reforming (57%). As with the previous molecule (DMP), results for the zirconate absorbents Na_2ZrO_3 and Li_2ZrO_3 were similar between them and to the ones for CaO*MO as can be seen in Table 4. For instance, hydrogen production rate (HR) for Na_2ZrO_3 and Li_2ZrO_3 were 16.4 and 15.1, respectively, only slightly reduced for Li_2ZrO_3. Equilibrium mols of CO followed the same trend, while CO_2 mols presented only a slight increase of the zirconate absorbents compared to those produced by calcined dolomite (0.005 compared to 0.0163 and 0.0097) and the same trend occurred with methane formation. Hydrogen concentration was essentially the same for the zirconates (99%) compared to the concentration produced by calcined dolomite (99.7%).

Similarly to the case for furfural reforming, VAI reforming using Li_4SiO_4 produced the lowest hydrogen production and higher byproduct concentrations (CO, CO_2 and CH_4). This was translated in a lower hydrogen concentration of only 94.4%. This behavior can be attributed to the limited thermodynamic nature of this absorbent as referenced above.

Therefore, as in the case for the three model molecules (furfural, DMP and vanillin) the above thermodynamic analysis for the absorption enhanced reforming of DMP leads to conclude that Na_2ZrO_3 and Li_2ZrO_3 are both promising alternate absorbents with comparable thermodynamics to CaO-based absorbents. Also, it is important to mention that DMP and VAI results showed higher hydrogen production and concentrations than those generated by the FUR model molecule. This behavior was attributed to the oxygen content in each bio-fuel fraction according to results reported by Lima da Silva and Müller [43] who compared several oxygenated hydrocarbons under the AESR reaction scheme and found the that higher hydrogen content in the product gas is directly related to the oxygen content in the fuel.

3.5 Carbon Formation

3.4.1 Carbon Formation for the Furfural Reforming System

Figure 28 shows the effect of steam to FUR molar ratio and temperature on the number of moles of carbon (graphite) produced in the steam reforming of furfural and through AESR using all the absorbents studied in the present work.

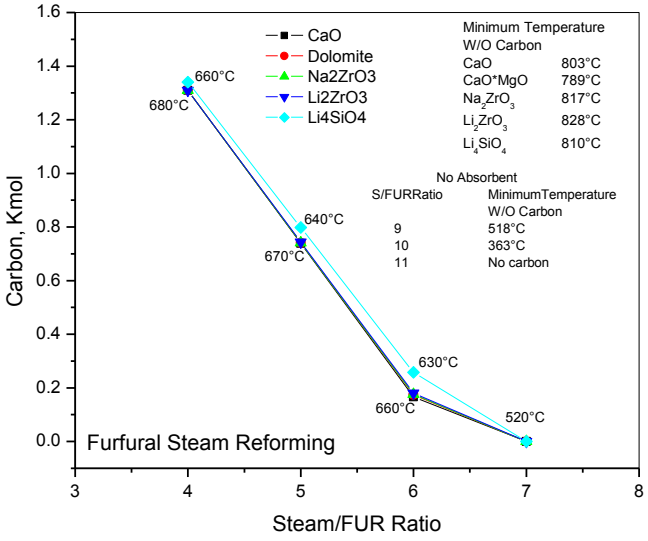

Figure 28. Equilibrium Maximum Carbon Formation for FUR Steam Reforming with Absorbents.

In this plot the maximum amount of carbon produced is plotted as a function of the S/FUR ratio from 4 to 7. In each data point the temperature where the maximum carbon formation was found is specified. Also, in this plot there are two tables. One specifies the minimum temperature reached without carbon formation for every type of CO_2 absorbent. The temperature in this table can be defined as the minimum temperature, necessary to inhibit carbon deposition at the minimum S/FUR ratio for each absorbent. The second table is devoted to the minimum temperature and S/FUR ratio found without carbon formation without the use of a CO_2 absorbent. Greater temperatures and S/FUR ratios will insure a carbon free operating region.

In this plot it is evident that without the use of a CO_2 absorbent carbon formation is favored (second table in Figure, no absorbent) at temperatures lower than 518°C with S/FUR ratio of 9. Also greater temperatures than 363°C will prevent carbon formation at S/FUR ratio of 10. Furthermore, a S/FUR ratio of 11 and greater will insure a carbon free operation.

On the other hand, the use of different CO_2 absorbents produced maximum carbon formation at the same temperatures and S/FUR ratios, with only the exception of Li_4SiO_4 that deviated from this behavior at slightly lower temperatures. Furthermore, for the other absorbents, greater S/FUR ratios than 6 will produce lower amounts of carbon. Carbon free operation can be found at S/FUR ratios greater than 7 and at temperatures higher than 520°C. The behavior related to the lower carbon formation found with the use of a CO_2 absorbent, is directly related to the reduction in CO content. Li [44] confirmed in his thermodynamic study, that graphite formation is suppressed with CO_2 absorption. According to this author, the Boudouard reaction:

$$2CO(g) = CO_2(g) + C(s) \qquad \Delta H°_{298} = -172.5 \text{ kJ/mol} \qquad (17)$$

is shifted towards the reverse Boudouard reaction because its equilibrium constant is related to the square of CO concentration.

3.4.2 Carbon Formation for the DMP Reforming System

Figure 29 shows the effect of S/DMP ratios and temperature on the number of moles of carbon generated under the steam reforming of DMP and through the AESR systems. Again in this scheme the maximum amount of carbon produced is plotted as a function of the S/DMP ratio from 10 to 13. In each data point the temperature where the maximum carbon formation was found is specified. Also, as in the case of furfural reforming it is clear that the use of a CO_2 absorbent produces a low tendency to deposit carbon. In order to insure carbon free operation without the use of an absorbent under this system a S/DMP ratio greater than 16.5 and temperatures higher than 335°C are needed.

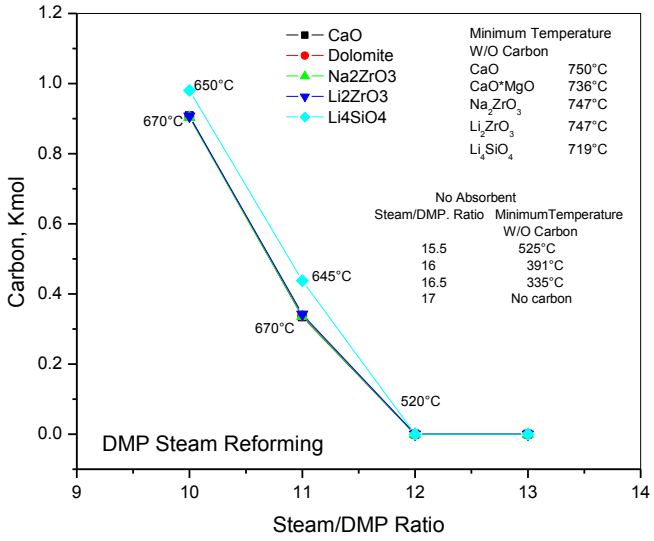

Figure 29. Equilibrium Maximum Carbon Formation for DMP Steam Reforming with Absorbents.

Also, in Figure 29 it can be observed that either CaO-based (CaO and CaO*MgO) and synthetic absorbents (Na_2ZrO_3, Li_2ZrO_3 and Li_4SiO_4) will avoid carbon formation at S/DMP ratios greater than 12.

3.4.3 Carbon Formation for the VAI Reforming System

Figure 30 presents results of the amount of carbon formation as a function of S/VAI ratios and temperature. Here, the maximum amount of carbon produced is plotted as a function of the S/DMP ratio from 8 to 11. In each data point the temperature where the maximum carbon formation was found is specified. Also, in vanillin reforming it is clear that the use of a CO_2 absorbent produces a low tendency to deposit carbon. Without the use of an absorbent, a minimum S/VAI ratio of 17 is needed in order to avoid carbon formation.

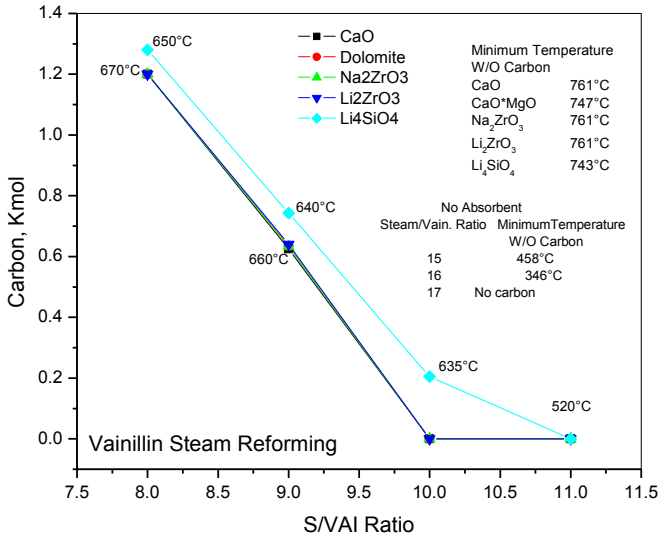

Figure 30. Equilibrium Maximum Carbon Formation for Vanillin Steam Reforming with Absorbents.

Also, in Figure 29 it can be observed that either CaO-based (CaO and CaO*MgO) and synthetic absorbents (Na_2ZrO_3, Li_2ZrO_3 and Li_4SiO_4) will avoid carbon formation at S/DMP ratios greater than 11 and temperatures greater than 520°C.

3.4.4 Kinetics Effects and Other Considerations in the AESR process

From the previous thermodynamic analysis it is clear that the CO_2 absorbent is the key component responsible for the enhanced effect towards the production of high purity hydrogen through the AESR of bio-oil. Several studies have shown that CO_2 capture kinetics are very important, in many cases being the rate limiting step [45-47]. In these studies results have shown that CO_2 removal at low partial pressures is critical in order to achieve high efficiency of the process and to reduce the reactor size. It has been reported that CaO presents high capacity and fast CO_2 kinetics, both at high and low CO_2 concentrations [45]. Even though, Li_2ZrO_3 have experimentally shown a fair performance at 100% CO_2, very slow kinetics were observed when the partial pressure of CO_2 was reduced to low levels (≈ 10% CO_2). The doping of the material with K enhanced the kinetics considerably, although, the doping resulted in a absorption capacity

decrease and this reduction was directly associated to the amount of doping agent [47]. Some researchers have related the doping effect to the formation of an eutectic molten carbonate at high temperatures, thus reducing the diffusion resistance of CO_2 on the acceptor [48]. Ochoa Fernandez et al. [47] have found that Li_4SiO_4 performed similar kinetics and capacity as K-doped Li_2ZrO_3, while Na_2ZrO_3 showed the fastest kinetics among its ceramic counterparts (Li_2ZrO_3 and Li_4SiO_4) comparable with the kinetics of CaO, even at the low partial pressures of CO_2. However, Na_2ZrO_3 has lower total capacity than CaO.

Other important consideration not accounted by thermodynamics is the kinetic performance of the absorbent at reduced CO_2 partial pressures, since the CO_2 partial pressure within the reactor environment at the normal enhanced absorption methane steam reforming conditions (SESMR) conditions is lower than 10% and in the present study (AESR of bio-oil model molecules) thermodynamics predicts a partial pressure in the range of 10-13% (wet basis). Therefore, the properties of the acceptor and its performance in this concentration range are of paramount importance to produce for a high hydrogen yield. For example, with slow absorption kinetics (as is the case of Li_2ZrO_3), long contact times are needed due to poor kinetics at working conditions and as a result, the working capacity of the process becomes poor compared to conventional steam reforming [49]. Consequently, there is the need of an absorbent capable to efficiently capture CO_2 at low partial pressures and having high absorption capacity.

In a recent study, a comparison of five different high-temperature CO_2 absorbents was performed under the absorption enhanced reforming of methane [47]. The results in that study showed that none of the acceptors completely fulfilled all the requirements for SESMR. That research concluded that CaO was the most favorable absorbent from the thermodynamic point of view leading to the highest H_2 yields. However, further development of the material is necessary in order to improve its stability. Also, they pointed out that Na_2ZrO_3 may be a good alternative due to the good kinetics and stability, but an increase in its total capacity is desirable.

Other important issues that are needed to be considered and that thermodynamics would not take into account are the ones related to the compatibility of the reforming catalyst and the CO_2 absorbent. Many studies have emerged that use a physical mixture of catalyst/absorbent without mayor drawbacks [8, 11, 14, 15, 34 and 41]. However some problems may arise due to the formation of mixed oxides of catalyst-absorbent phases especially at high temperatures and with synthetic ceramic absorbents. However, a recent research trend is to combine the catalyst and the absorbent into one single particle to avoid this problem [50].

3.5 Optimal Operating Conditions for AESR process

For furfural as a model compound, under the AESR system, it can be seen that it is possible to obtain a hydrogen concentration of ≈ 99% purity at 1 atm, 550°C and S/FUR = 24. Conditions found in the present thermodynamic analysis pointed out that for furfural reforming S/FUR = 24 and 550°C will provide a HR of 9.9 and a hydrogen concentration as high as 99.5%. Otherwise, for the steam reforming of DMP optimal conditions found were S/DMP = 45 and 600°C, which produced a hydrogen concentration of 99%. Furthermore, for the steam reforming of VAI optimal conditions found were S/VAI = 39 and 450°C, which produced a hydrogen concentration of 99.9%. Also, it is worth to mention that there is a compromise related to the use of steam, since the excessive use of this, will eventually be reflected in detrimental of the thermal efficiency of the process. Therefore, the experimental evaluation of these systems are needed in order to verify and/or adjust equal or lower S/fuel ratios to avoid a reduction of the thermal efficiency of the process and consequently an uneconomical operation of these reactions systems towards the utilization of bio-oil for the efficient production of hydrogen.

4.0 CONCLUSIONS

Thermodynamic analysis of steam reforming of bio oil model molecules, 2,4-dimethylphenol (DMP, C_8H_9OH), furfural (FUR, $C_5H_4O_2$) and vanillin (VAI, $C_8H_8O_3$) with and without CO_2 absorbents were carried out to determine favorable operating conditions to produce a high purity

H_2 gas product. CO_2 absorbents employed include; CaO, CaO*MgO, Na_2ZrO_3, Li_2ZrO_3 and Li_4SiO_4

Results indicate no carbon formation for S/bio-oil model molecules ratios equal or greater than stoichiometric values for their corresponding steam reforming reactions. However, for the furfural system using CO_2 absorbents, carbon free operation can be found at S/FUR ratios greater than 7 and temperatures higher than 520°C. While, for DMP reforming carbon free operation is achieved at S/DMP ratios greater than 12 and temperatures higher than 520°C. Also, carbon formation is avoided for VAI reforming using CO_2 absorbents at S/VAI ratios greater than 11 and temperatures higher than 520°C. In general, carbon formation is suppressed with CO_2 absorption compared to conventional reforming operation for all model molecules studied.

The use of a CO_2 absorbent resulted in an increase in HR (mols H_2/mols model molecule) and H_2 purity. This enhancement under the furfural reforming system produced a 16.2% increase in hydrogen production with respect to the conventional reforming and the hydrogen concentration was increased from 62 to 99%. Otherwise, with the DMP reforming system a 45% increase in hydrogen production was reached, while the hydrogen concentration increased from 63 to 99%. Furthermore, vanillin reforming achieved an increase of 111% with respect to the conventional reforming and an increase in hydrogen concentration from 57 to 99.9%. Under optimal operating conditions for AESR process it is possible to produce a hydrogen concentration of ≈ 99% purity at 1 atm, 550°C and S/FUR = 24 for furfural reforming, while this also can be achieved at 600°C and S/DMP = 45 for DMP reforming. For VAI reforming optimal operating conditions under the AESR are S/VAI = 39 and 450°C. The order from higher to lower hydrogen production based on model molecule compound wasjj: VA > DMP > FUR. For all model molecules CaO and CaO*MgO showed similar results with high levels of hydrogen production rates and concentrations, Na_2ZrO_3 and Li_2ZrO_3 resulted only in slightly lower values than CaO, while Li_4SiO_4 showed significantly lower values than CaO. The order from higher to lower hydrogen

production and concentration based on each CO_2 absorbent was as follows: CaO > CaO*MgO > Na_2ZrO_3 > Li_2ZrO_3 > Li_4SiO_4.

The AESR technology represents a promising low-temperature process for high-quality H_2 production with low propensity to carbon formation. Furthermore, the use of low temperatures could bring beneficial effects on the life of the catalysts and the construction materials of the reformers as well as in substantial energy savings. Besides these technological aspects, other advantages of the AER are expected, such as easy CO_2 sequestration. In this case, the use of bio-oil in conjunction with AESR could be a potentially viable carbon-negative process

Finally, Na_2ZrO_3 and Li_2ZrO_3 can be considered as promising alternate absorbents with comparable thermodynamics to the reference CaO absorbent for bio oil reforming applications in the present work. However, the limited durability of CaO and CaO*MgO absorbents make these zirconate materials ideal absorbents to be used under the AESR system. Finally, from the two zirconates, Na_2ZrO_3 is the one that presents greater kinetics and superior stability. Therefore, Na_2ZrO_3 should be considered as a high potential absorbent under the AESR of bio oil for future experimental evaluations.

5.0 REFERENCES

[1] Q. Zhang, J. Chang, T. Wang, Y. Xu, *Energ. Convers. Manage*., **48**, 87-89 (2007)

[2] A. Seda, K. Mustafa, K. Ahmet, *Int J Hydrogen Energy*, **34**, 1752 – 1759 (2009)

[3] C. Wu, M. Sui, Y. Yan, *Chem. Eng. Technol*., **31**, 1748-1753 (2008)

[4] E. Vagia, A. Lemonidou, *Int J Hydrogen Energy*, **32**, 212 – 223 (2007)

[5] C. Wu, Y. Yan, T. Li, W. Qi, *Chin J Process Eng*, **7**, 1114-1119 (2007)

[6] Brun-Tsekhovoi AR, Zadorin AN, Katsobashvili YR, Kourdyumov SS. The process of catalytic steam-reforming of hydrocarbons in the presence of carbon dioxide acceptor. In: Proceedings of the world hydrogen energy conference, vol. 2. New York: Pergamon Press, 885–900 (1986).

[7] J. R. Hufton, S. Mayorga, S. Sircar, *AIChE J*, **45**, 248–256 (1999).

[8] B. Balasubramanian, A. Lopez-Ortiz, S. Kaytakouglu, D. P. Harrison, *Chem Eng Sci*, **54**, 3543–3552 (1999).

[9] J. C. Abandes, *Chem Eng J*, **90**, 303–306 (2002).

[10] R. Davda, J. Shabaker, G. Huber, R. Cortright, J. Dumesic, *Appl Catal B: Environ*, 56, 171-186 (2005)

[11] K. B. Yi, D. P. Harrison, *Ind Eng Chem Res*, **44**, 1665–1669 (2005).

[12] M. Kato, S. Yoshikawa, K. Nakawaga, *J. Mater Sci. Lett.*, **21**, 485 (2002).

[13] A. López, N. Pérez, A. Reyes, D. Lardizábal, *Sep. Sci. Technol.* **39**, 3563–3579 (2004)

[14] C. M. Kinoshita, S. Q. Turn, *Int J Hydrogen Energy*, **28**, 1065–71 (2003).

[15] A. A. Iordanidis, P. N. Kechagiopoulos, S. S. Voutetakis, A. A. Lemonidou and I. A. Vasalos, *Int J Hydrogen Energy*, **31**, 1058-1065 (2006).

[16] C. Rioche, S. Kulkarni, F. C. Meunier, J. P. Breen, R. Burch. *Appl Catal B Environmental*, **61**, 130–139 (2005).

[17] F. Bimbela, M. Oliva, J. Ruiz, L. Garcia, J. Arauzo, *J Anal Appl Pyrolysis*, **79**, 112–1120 (2007).

[18] M. Marquevich, S. Czernik, E. Chornet, D. Montane, *Energy & Fuels*, **13**, 1160–1166 (1999).

[19] D. Wang, D. Montane, E. Chornet, *Appl Catal A Gen*, **143**, 245–270 (1996)

[20] S. Yaman, Energy Conv Manag, **45**, 651–671 (2004).

[21] A. C. Basagiannis, X. E. Verykios, *Int J Hydrogen Energy*, **32**, 3343–3355 (2007).

[22] C. Resini, L. Arrighi, M. C. H. Delgado, M. A. L. Vargas, L. J. Alemany, P. Riani, *Int J Hydrogen Energy*, **31**, 13–19 (2006).

[23] D. C. Rennard, P. J. Dauenhauer, S. A. Tupy, L. D. Schmidt, *Energy & Fuels*, **22**, 1318–1327 (2008).

[24] P. N. Kechagiopoulos, S. S. Voutetakis, A. A. Lemonidou, I. A. Vasalos, *Catal Today*, **127**, 246–255 (2007).

[25] S. Adhikari, S. Fernando, S. R. Gwaltney, S. D. Filip To, R. M. Bricka, P. H. Steele, *Int J Hydrogen Energy*, **32**, 2875–2880 (2007).

[26] A. Ishihara, E. W. Qian, I. N. Finahari, I. P. Sutrisna, T. Kabe, *Fuel*, **84**, 1462–1468 (2005).

[27] M. Ni, D. Y. C. Leung, M. K. H. Leung, *Int J Hydrogen Energy*, **32**, 3238–3247 (2007).

[28] S. Jarungthammachote, A. Dutta, *Energy Convers. Manage*, **49**, 1345–1356 (2008).

[29] A. Roine, Chemical reaction and equilibrium software with extensive thermo-chemical database. Outokumpu HSC 6.0 Chemistry for windows (2010).

[30] Y. Chang-Feng, H. En-Yuan, C. Chi-Liu, *Int J Hydrogen Energy*, **35**, 2612-2616 (2010).

[31] M. R. Mahishi, D. Y. Goswami, *Int J Hydrogen Energy*, **32**, 2803–2808 (2007).

[32] C. F. Yan, E.Y. Hu, C. L. Cai, R. Hu, Experimental research on hydrogen production from bio-oil aqueous fraction. 17th World Hydrogen Energy Conference, Brisbane, Australia.

[33] S. Aktaş, M. Karakaya, A. K. Avc, *Int J Hydrogen Energy*, **34**, 1752-1759 (2009).

[34] A. Lopez-Ortiz, D. P. Harrison, *Ind. Eng. Chem. Res.,* **40**, 5102 -5109 (2001)

[35] A. Silaban, D. P. Harrison, *Chem Eng Comm*, **47**, 149-162 (1996)

[36] C Han, D. P. Harrison, *Sep Sci Technol*, **32**, 681-697 (1997)

[37] A. Bandi, M. Specht, P. Sichler, N. Nicoloso, In situ gas conditioning in fuel reforming for hydrogen generation. 5th International Symposium on Gas Cleaning at High Temperature. Morgantown West Virginia. (2002). Available at: http://www.zsw-bw.de/en/docs/research/REG/pdfs/REG_5th_ISGC_2002.pdf.

[38] Y. Ding, E. Alpay, *Process Saf Environ Prot*, **79**, 45-51(2001).

[39] K. Nakagawa, T. J. Ohashi, *J Electrochem Soc*, **145**, 1344-1346 (1998).

[40] M. Kato, S. Yoshikawa, K. Essaki, K. Nakagawa, Novel CO_2 absorbents using lithium-containing oxides. In Toshiba Corporation. INTERMAC, Japan Electric Measuring Instruments Manufacturers' Association, Joint Technical Conference.; **SE-3,** 1021 (2001).

[41] E. Ochoa-Fernández, C. Lacalle-Vilà, T. Zhao, M. Rønning, D. Chen, *Stud Surf Sci Catal*, **167**, 159-164 (2007).

[42] J. P. Jakobsen, E. Halmøy, *Energy Procedia*, **1**, 725-732 (2009).

[43] A. Lima da Silva, I. L. Müller, *Int J Hydrogen Energy*, **36**, 2057-2075 (2011)

[44] M. Li, *Int J Hydrogen Energy*, **34**, 9362-72 (2009).

[45] D. P. Harrison, "The Role of Solids in CO_2 Capture: a Mini Review", Proceedings of the 7th International Conference on Greenhouse Gas Control Technologies Vancouver, Canada 1101-1106, (2004).

[46] S. Stendardo, P. U. Foscoloa, *Chem Eng Sci*, **64**, 2343-2352 (2009).

[47] E. Ochoa-Fernández, G. Haugen, T. Zhao, M. Rønning, I. Aartun, B. Børresen, E. Rytter, M. Rønnekleivb, D. Chen, *Green Chem*., **9**, 654-662 (2007).

[48] R. Xiong, J. Ida, Y. S. Lin, *Chem. Eng. Sci*., **58**, 4377-4385 (2003).

[49] E. Ochoa-Fernández, H. K. Rusten, H. A. Jakobsen, M. Rønning, A. Homen and D. Chen, *Catal. Today*, **106**, 41-46 (2005).

[50] M. H. M. Halabi, "Sorption Enhanced Catalytic Reforming of Methane for Pure Hydrogen Production Experimental and Modeling", Ph. D. Dissertation, Technische Universiteit Eindhoven, ISBN: 978-90-386-2454-9, (2011)